Design and Synthesis of Probes for Detection of Protein-Protein Interaction and RNA Localization

By

Jeremy Adam Ryan

B.A. Chemistry and Biology

Saint Mary's College of Maryland

Submitted to the Department of Chemistry in Partial Fulfillment of the Requirements for the Degree of Master of Science in Organic Chemistry

at the

Massachusetts Institute of Technology

August 2005
[September 2005]

Signature of Author .....
Department of Chemistry
August 31, 2005

Certified by.....
Alice Y. Ting
Department of Chemistry
Thesis Advisor

Accepted by.....
Robert W. Field
Chairman
Committee on Graduate Students

Design and Synthesis of Probes for Detection of Protein-Protein Interaction and RNA Localization

By

Jeremy A. Ryan

Submitted to the Department of Chemistry
On August 31, 2005 in Partial Fulfillment of the
Requirements for the Degree of Master of Science in
Organic Chemistry

ABSTRACT

The use of the ketone biotin – benzophenone-biotin hydrazide system for detecting the formation of cyan fluorescent protein and NF-kappaB p50 dimers was assessed. A series of benzophenone-based probes were synthesized and tested for photocrosslinking activity to investigate the efficiency of photocrosslinking in these systems.

Three series of small molecule probes were synthesized for the selection of ribozymes from a random sequence pool. Solid-phase immobilized fluorescein and fluorescein phosphates were synthesized for the indirect selection of a fluorescein phosphatase ribozyme. A corresponding thiophosphate analog was created for the in-gel selection of a thiophosphatase ribozyme via APM-PAGE. Finally, a series of fluorescein-nucleoside phosphate conjugates was designed and synthesized for use in the solution phase preparation of a fluorogenic ribozyme substrate, and later immobilization of this substrate on a silyl resin for direct ribozyme selection.

Thesis Supervisor: Alice Ting
Title: Associate Professor of Chemistry

Dedicated to my family and friends.

It is by their strength and encouragement
that I have come this far.

Table of Contents

Acknowledgements

It's hard to know where to begin in giving thanks to those who've helped me in the past few years. I could go on for pages just with the names of everyone who has lent some bit of their strength or their expertise to me during my work. However, I'll do my best to keep it brief. I apologize if anyone is somehow left out though please do not think yourselves forgotten.

The first people I would like to thank are my coworkers in the Ting lab. I've worked with some wonderful people over the years in a number of very different workplaces, but I have to say that they are among the best people I have worked with yet. Their energy and spirit is infectious, and that has pushed me along through many days when I might have hung up my lab coat. While there is no one in the lab who hasn't helped me in some way, I want to recognize Chi Wang Lin and Marta Fernandez Suarez in particular. In some ways, you two have been my guardian angels in the lab. I could never thank either of you enough with mere words for all the advice and encouragement you've given me. I'd also like to thank Eric McNeill. You're the first student I've ever trained in a laboratory environment, and I have to say that it was an honor to do so. Rarely have I met such a motivated person, and you've learned so much in such a short time. I'm looking forward to seeing your career develop.

I've not been without my share of guardians outside the lab. To Jonah, Jen, Chris, and all the Northeast crew, thank you for many good meals, laughs, and evenings together. I think like would have been quite difficult without you here to help me along. You've all been my family away from home, and my connection to you all makes me hesitant to ever leave this part of the country.

Next in line, I should mention Prof. Ting herself. I wouldn't be writing this without the opportunities she provided me. I'm not sure we always saw eye-to-eye, but I certainly learned a lot from her and working in her lab. My skills as a researcher benefited greatly from her scrutiny.

Last, but not least in any respect, I must thank my family. I'm not sure how much of my work they understand, but the one thing I always know is that they are behind me no matter what research I engage in. I could not have come this far without their constant encouragement and boundless love. There is nothing else in this world that makes me happier than thinking of them, and I am proud to be a Ryan.

Chapter 1: Detection of p50 dimerization by photocrosslinking

Introduction

Protein-protein interactions play a critical role in the function of a cell. A vast network of interactions mediates critical functions such as signal transduction, gene expression, and intracellular transport to name a few. Study of this network, is essential for understanding normal cellular function and gaining insight to correct the imbalances that lead to disease states. A critical step in exploring this intricate web is the identification of interacting factors.

A variety of methods has been developed for studying interactions between proteins. The use of immunoprecipitation is a well-accepted method for detecting these interactions[1]. While quite reliable, the method requires the generation of multiple antibodies and requires a large number of controls to rule out false positives. Furthermore, this method yields data that represents an average over a cell population while sacrificing both spatial and temporal information. Alternatively, immunofluorescence staining allows for detection of the protein with retention of spatial information, but can only demonstrate protein co-localization within 200-500 nm[2-4].

Protein complementation and fluorescence resonance energy transfer (FRET) assays provide higher spatial resolution of the protein interactions. Examples of protein complementation systems include the yeast 2-hybrid and split-GFP methods. The yeast 2-hybrid method takes advantage of fusions to transcription factor fragments to modulate the expression of a reporter. The DNA binding domain and transcriptional activator domain are fused to the two proteins suspected of interacting. If they interact, the two domains are brought together and trigger the expression of the reporter. However, this method gives both false positives or negatives when the transcription factor fragments induce interaction or the fusions prevent interaction of the fragments respectively. Furthermore, the system is restricted to proteins localized within the nucleus. [1] The split GFP system, in which each protein of interest is fused to a fragment of green fluorescent protein (GFP), allows for detection outside the nucleus by using the recombination and folding of GFP fragments to form a fluorophore[1, 5]. Unfortunately, the monitoring of transient interactions is hampered by the irreversible nature of this folding event[1]. Like

the yeast 2-hybrid approach, it is also possible for the GFP fragments to induce interaction, thereby creating false positives. FRET relies on the proximity of a donor and acceptor fluorophore to produce a signal. As the intensity of the FRET signal is proportional to the distance between the donor and acceptor[6], the system can be used to detect the interaction of two proteins fused to the fluorophores. All three approaches use rather large protein labels, and could potentially alter protein localization and behavior, and hamper normal interaction of the fused proteins[5, 7]. The use of a smaller tag would reduce the chances of disrupting wild-type behavior. Small molecule labels, such as crosslinking moieties capable of trapping interacting proteins, could replace these systems, but need a method for directing them in a site-specific manner.

Several methodologies are available for site-specific labeling of proteins using small peptide tags. A Texas Red binding peptide was selected from a phage library to result in tags less than 50 amino acids capable of fluorescent protein labeling[8]. The His_6 – Ni-NTA interaction has also been used to fluorescently label His_6-tagged proteins[9]. Another six amino acid tag containing a CCXXCC motif allows for the binding of biarsenical fluorophores[10]. While an improvement over current labeling strategies, all these methods lack covalent attachment between the protein and the label, which can result in loss of signal due to dissociation. A more optimal solution should feature covalent linkage to the protein.

Biotin ligase (BirA) covalently labels proteins bearing a 15 amino acid tag, the acceptor peptide (AP). Our lab recently demonstrated the labeling of proteins *in vitro* as well as on cell surfaces with a ketone analog of biotin (KB)[11]. Ketone biotin can then be labeled with hydrazide probes including the bi-functional probe BPBio-hydrazide that bears a benzophenone (BP) group for photocrosslinking and biotin (Bio) for product capture and detection. The utility of this methodology in labeling proteins site-selectively has been demonstrated, but its second function in photo cross-linking interacting proteins has yet to be shown. This would provide a way to 'lock-down' proteins interacting with the tagged protein for later identification. To demonstrate this function, a well-characterized protein-protein interaction was chosen.

The NF-κB family of transcription factors serves a wide variety of roles in healthy and diseased states. Even though they are most commonly known for their roles

in the regulation of elements of immunity and inflammation[12-15], excessive activation of these factors has also been linked to cancer[16] and chronic inflammatory diseases[17]. Normally masked by inhibitory proteins in the cytosol, a variety of stimuli can trigger activation and cause NF-κB to dimerize and translocate to the nucleus where they may regulate gene expression. Among all the NF-κB factors, we chose p50 based on the availability of the crystal structure of the interacting proteins[13, 18] as well as the binding affinities for the dimerization event under a variety of conditions[19, 20]. These data made p50 a good choice for the demonstration of the photo cross-linking potential of the KB-BPBio labeling methodology.

Results

Cyan fluorescent protein (CFP) bearing a C-terminal acceptor peptide (CFP-AP) as well as the CFP mutant bearing a lysine to alanine mutation in the AP (CFP-Ala) was recombinantly expressed from pRSETB. The p50-AP gene was amplified by PCR from the p50 protein in pET15b[18] with primers to introduce an N-terminal BamHI site and a C-terminal AP tag, stop codon, and EcoRI site. The resulting PCR product was gel purified and ligated into a BamHI / EcoRI / CIP digest of pRSETB. The ligation product was transformed into DH5α, and clones selected for sequencing. The p50-Ala mutant was obtained from p50-AP by site-directed mutagenesis and confirmed by sequencing.

Expression of all proteins was conducted in *E. coli* strains BL21(DE3) or JM109. CFP-AP and CFP-Ala in pRSETB expressed well in both strains as did recombinant biotin ligase (BirA) in cloned pBTac. All proteins were purified by a Ni-NTA column. In contrast, only low levels of expression were found for both p50 proteins in pRSETB. Attempts to optimize induction time, IPTG concentration, bacterial strain, growth medium, and temperature did not improve protein yield. The wild-type protein, which was cloned in pET15b, was found to express well. Sufficient protein was obtained from multiple preparations to conduct experiments, and all AP-tagged proteins used herein are from pRSETB vectors. However, a means to improve protein yield for later work was still sought.

A search of the literature found that most successful expressions of p50 proteins *in vitro* had been obtained when p50 was cloned in pET vectors. Thus, the gene was transferred to a new vector. pET21b was chosen as it contained both BamHI and EcoRI sites in the correct orientation as well as ampicillin resistance. Use of this plasmid, however, changed the position of the His_6-tag used for Ni-NTA purification from N-terminal to C-terminal and required removal of the C-terminal stop codon used in pRSETB. Transfer of the gene was completed by BamHI / EcoRI double digest of both vectors, and gel purification of both insert and vector, followed by ligation. Plasmids were confirmed by sequencing and site-directed mutagenesis was performed to remove the stop codon and bring the His_6-tag in frame. Following mutagenesis, the new plasmids were again confirmed by sequencing.

As *E. coli* normally express their own BirA, AP-tagged proteins are expressed with a significant level of pre-biotinylation. This pre-biotinylated material must be removed to avoid false positives during biotin detection. Streptavidin-agarose was used to capture biotinylated protein following Ni-NTA purification to yield purified AP-tagged proteins. The efficiency of debiotinylation and integrity of the AP tag was tested using a biotinylation assay.

BirA also required processing after purification as the biotin-AMP ester is retained in the active site and co-purifies with BirA. This is easily removed by allowing the enzyme to catalyze its reaction in the presence of excess synthetic AP, followed by repurification by Ni-NTA column. A more rigorous treatment by including ATP along with AP was used later to ensure complete removal of possible biotin sources.

In the biotinylation assay, AP-labeled proteins were exposed to excess biotin in the presence of 1 μM BirA with or without the addition of ATP. Detection of the biotinylated proteins following SDS-PAGE and western blot using streptavidin-HRP revealed labeling only in the presence of ATP (Figure 1-1A).

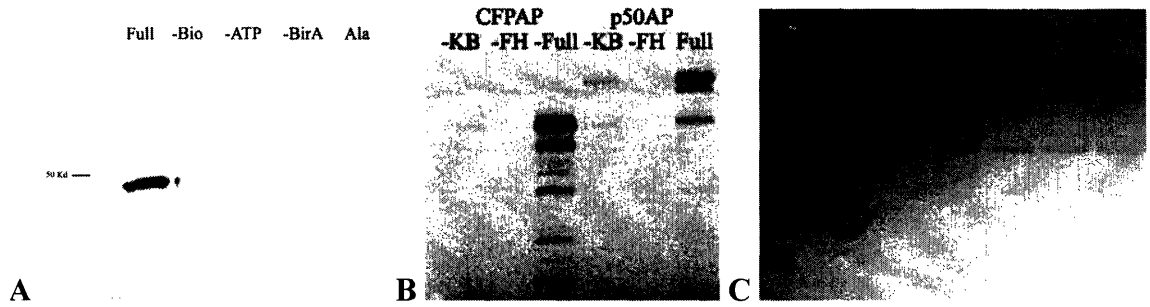

Figure 1-1: *A: Streptavidin-HRP western blot of p50AP background biotinylation test. –bio lacks biotin, -ATP lacks ATP, -BirA lacks biotin ligase, and Ala lacks the AP lysine* ***B****: In-gel fluorescence detection of fluorescein hydrazide is dependent on ketone biotin incorporation and presence of hydrazide. –KB lacks ketone biotin and –FH lacks fluorescein hydrazide* ***C:*** *Coomassie stain of fluorescein hydrazide gel. CFP and BirA appear at 37 kD while p50-AP appears just below 50 kD. The observed fluorescence signal is not due to uneven protein loading.*

Equal protein loading was verified by Ponceau staining. Removal of pre-biotinylated proteins and any biotin-AMP appeared complete as no background was detected in –ATP lanes. The AP-tag was also accessible to BirA as biotin was incorporated when ATP was available.

Once all AP-proteins and BirA were verified sufficiently pure free of biotin contamination, ketone biotinylation and hydrazide conjugation were tested. AP-proteins were incubated in the presence of BirA and racemic ketone biotin (KB) for three hours at pH 8.2 in the presence of ATP to allow for labeling of the AP tag. The reaction was then acidified to pH 6.2 to aid in hydrazide conjugation, and incubated with the fluorescein hydrazide (FH) overnight. The resulting hydrazide adduct was reduced at 4 °C for 1.5 hours prior to SDS-PAGE. Fluorescein was then detected in-gel on a STORM fluorescence imager (Figure 1-1B). Thereafter, Coomassie staining was employed to reveal protein loading (Figure 1-1C). Only proteins in the presence of both KB and FH were labeled.

Labeling was then repeated using a benzophenone-biotin hydrazide probe (BPBio, Figure 1-2A). Ketone biotin labeling and hydrazide conjugation were conducted as previously described, with BPBio hydrazide replacing fluorescein hydrazide. SDS-PAGE

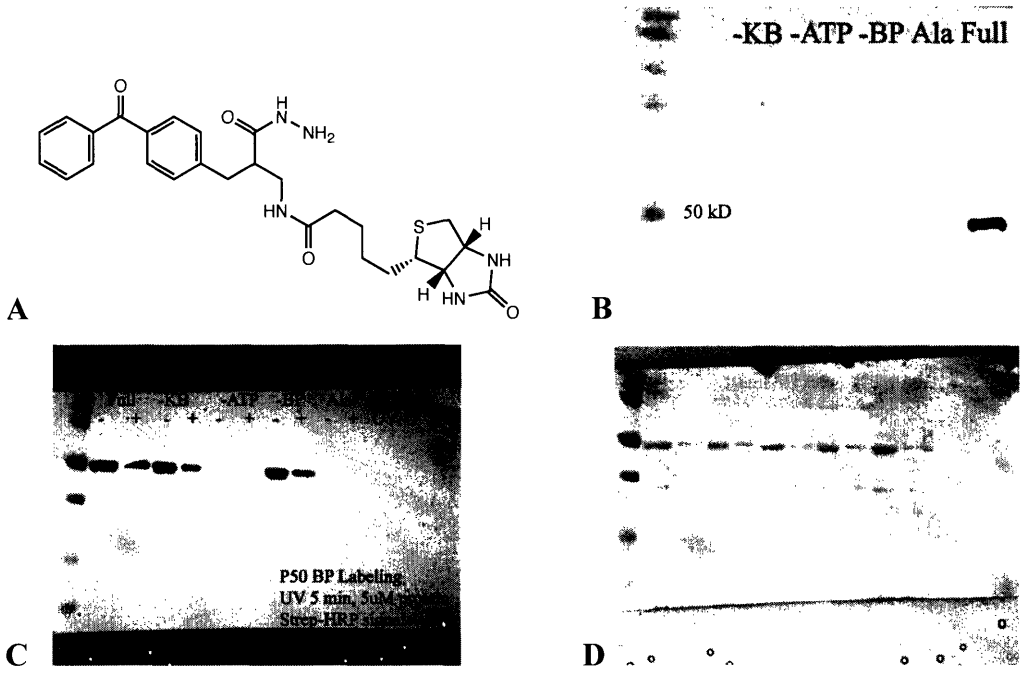

Figure 1-2: A: *Structure of BPBio hydrazide probe* ***B:*** *Streptavidin-HRP blot of p50 labeled with KB and BPBio-Hydrazide. Full contains all components for labeling, negative lanes indicate the omitted component. Ala represents the Lys to Ala mutant in the AP* ***C:*** *Streptavidin-HRP blot of p50 labeled by BPBio hydrazide and subjected to UV irradiation to trap dimmers. + Indicates a UV irradiated sample* ***D:*** *Ponceau stain of BPBio-labeled p50 blot. Lover loading in UV lanes is likely due to crosslinking to the container walls during irradiation*

followed by Western blot and streptavidin-HRP development (Figure 1-2C) allowed for visualization of the labeled proteins. An ATP-dependent labeling pattern was consistently observed over many repeated labeling experiments. Exposure to the full reaction conditions generated the strongest labeling, but significant background labeling was observed in the absence of ketone biotin or BPBio hydrazide.

The high background labeling observed in BPBio labeling was initially attributed to biotin contamination. AP-labeled proteins were subjected to additional streptavidin-agarose columns, BirA was reacted a second time with synthetic AP and ATP, and BPBio hydrazide was repurified by HPLC. Repetition of the labeling using the re-purified reagents still generated this labeling pattern. However, reducing the protein concentration 1000-fold resulted in a clean labeling pattern showing the expected dependence on all components of the labeling (Figure 1-2B).

The ability to cross-link interacting proteins was also examined. BPBio labeled samples were irradiated with long wave UV light on ice for 5-30 minutes prior to SDS-PAGE and western blot. Evidence of cross-linking was then assayed by streptavidin-HRP or silver staining. The BPBio hydrazide probe was unable to generate any significant level of cross-linked proteins under these conditions. Earlier tests with ketone biotinylation and fluorescein hydrazide labeling suggested that incorporation of ketone biotin or hydrazide conjugation ruled out lack of incorporation of either KB or the hydrazide probe. To test the cross-linking event itself, a second series of benzophenone probes were synthesized.

Benzophenone probes for general labeling as well as site specific labeling were prepared from commercially available compounds. Benzoylbenzoic acid was converted to the NHS ester by carbodiimide activation of the carboxylic acid using EDC-HCl. The benzophenone NHS ester (BP-NHS) was then reacted with either hydrazine to generate the corresponding hydrazide (BP-Hyd) or with 4-aminobutryic acid to add a flexible linker to the probe. The carboxylic acid was again activated with EDC-HCl in the presence of NHS to form the benzophenone-linker-NHS ester (BP4AB-NHS). As earlier, this was reacted with hydrazine to form the hydrazide (BP4AB-Hyd). All compounds used for protein labeling were HPLC purified prior to use.

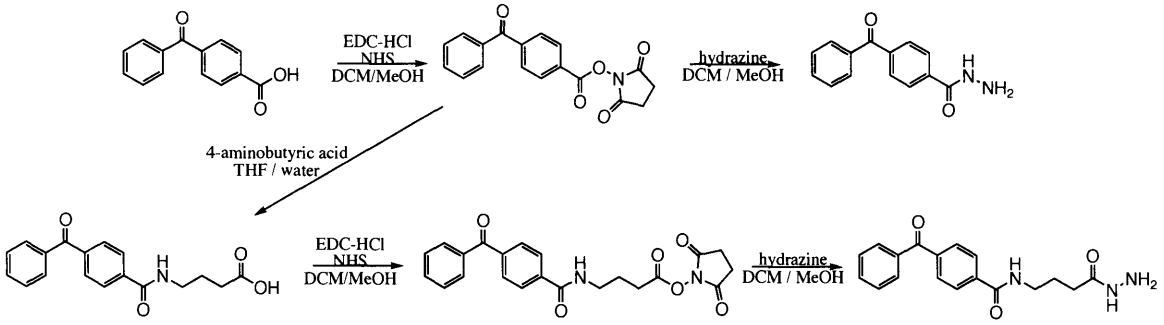

Scheme 1-1: *Synthesis of benzophenone NHS esters and hydrazides*

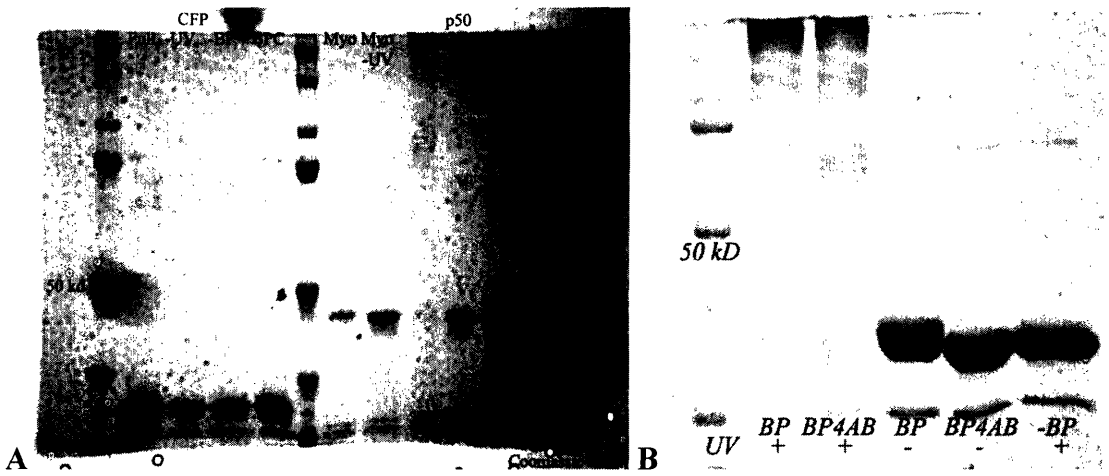

Figure 1-3: A: *Coomassie stain of BP-NHS ester labeling and crosslinking of CFPAP and p50AP – indicated the labeling component omitted and BPC is the benzophenone carboxylic acid* ***B:*** *Coomassie stain of CFPAP cross-linking using BP-NHS or BP-linker-NHS (BP4AB) + indicates UV irradiated samples.*

Non-specific labeling and cross-linking was first examined in CFP and p50. Concentrated stocks of both CFPAP and p50AP proteins were treated with 5 equivalents of either benzophenone NHS ester or benzophenone-linker NHS ester. Samples were UV irradiated on ice and analyzed on SDS-PAGE with Coomassie staining. Exposure to the NHS esters followed by UV irradiation generated a faint, higher weight band for both CFPAP and p50AP corresponding to the dimer (Figure 1-3A). Larger, higher order complexes were also detected for CFPAP, and were more prominent when the BP-NHS ester was employed. Some cross-linking was also noted when the parent benzophenone carboxylic acid was used. Dialysis of the proteins before UV irradiation was used to reduce this labeling without success. This background may be generated by hydrophobic interactions between the probe and the protein, followed by multiple cycles of excitation and radical recombination. As dimers were detected by photocrosslinking using these benzophenone probes, the site-specific hydrazide variants were then examined.

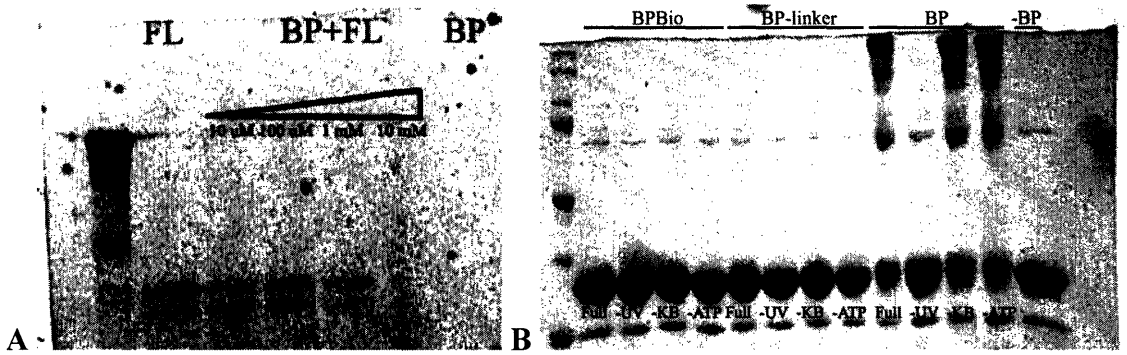

Figure 1-4: ***A:*** *In-gel fluorescence image demonstrating competition of fluorescein hydrazide by increasing concentrations of benzophenone hydrazide on KB-labeled CFPAP.* ***B:*** *Coomassie stain of CFPAP subjected to hydrazide labeling. Hydrazide probes used are indicated across the top and –BP designates no hydrazide present.*

Prior to cross-linking experiments with the BP-hydrazides, we determined whether they reacted with ketone biotin. To examine this, CFPAP was labeled with ketone biotin, and treated with 1 mM fluorescein hydrazide in the presence of increasing concentrations of BP-hydrazide (Figure 1-4A). The intensity of fluorescein labeling remained unchanged until the concentration of BP-hydrazide equaled that of fluorescein hydrazide. A ten-fold excess of BP-hydrazide abolished fluorescein labeling. These data suggest that the benzophenone hydrazide can label ketone biotin.

As CFPAP was available in higher concentration than p50AP, it was used in preliminary experiments for hydrazide conjugation and cross-linking tests. CFPAP was subjected to ketone biotin labeling followed by hydrazide conjugation and reduction. All three available hydrazide probes were examined in this assay. No cross-linking was observed in the absence of UV irradiation, and only BP-hyd was capable of cross-linking dimers. However, this cross-linking event was not dependant on ketone biotinylation. It likely arises from the same phenomenon responsible for labeling in the presence of the benzophenone carboxylic acid. As expected, UV irradiation in the absence of a benzophenone source did not produce labeling.

Discussion

The dimerization domain of NF-κB p50 was successfully expressed bearing both an N-terminal His_6 tag and C-terminal AP tag. While the expression of this protein from the pRSETB plasmid was not particularly high, sufficient protein was collected for use in assays. Further optimization of protein expression was achieved by transferring the gene to pET21b(+), and is recommended for further work with p50 as it results in much higher yield of protein.

The accessibility and functionality of the AP tag and the ketone biotin labeling system were verified by a number of assays. Successful labeling of the AP tag with biotin demonstrates both the accessibility of the AP tag as well as the ability of BirA to recognize it within the fusion. Background signals due to pre-biotinylation *in vivo* as well as trapped biotin-AMP ester copurified with BirA were readily removed by treatment with streptavidin-agarose or synthetic AP, respectively.

Biotin can be replaced by ketone biotin for use with hydrazide probes with only minor procedural modifications[11]. As streptavidin cannot detect ketone biotinylation with the amount of protein used in this assay, the ketone labeling was instead detected by fluorescein hydrazide (FH). By allowing FH to react with the ketone, fluorescein-labeled protein could be detected in a KB-dependent manner. Furthermore, the ketone-biotinylated product was detected using the BP-biotin hydrazide probe, allowing for detection by streptavidin-HRP. This labeling was dependent on the presence of all labeling components, including ATP and the presence of the AP lysine. Thus the p50-AP can be successfully labeled in the same manner as GFP and EGFR.[11]

In the absence of DNA, higher p50 concentration is required for dimerization. Analytical centrifugation data estimates the dissociation constant in the low micromolar range[21]. Thus, protein concentrations from 5-20 μM in p50 were used for crosslinking assays. At these concentrations, however, a higher background was noted in the detection of the BP-Bio probe, particularly in –KB and –BP lanes. Given the high loading of protein, it is possible that streptavidin will be able to weakly bind to ketone biotin and give rise to the weaker background signal in –BP samples. Trace levels of biotin in the BP-Bio probe may be responsible for the stronger background noted in the –KB lane. As

multiple purifications were unable to eliminate this signal, it is possible that the free biotin is due to slow degradation of BP-Bio. The use of EDTA to quench BirA activity prior to BPBio addition was also unable to reduce this background. These background signals, however, should not contribute to any photocrosslinking products as the previous assays have shown that the hydrazide probe, and hence the benzophenone, are only incorporated when all labeling components are present.

When BP-Bio labeled samples were irradiated at >320 nm at 0 °C for 2-30 minutes, no crosslinked products were observed. Neither silver staining (data not shown) or streptavidin-HRP showed any bands corresponding to dimer or higher-order products. As probe incorporation had already been established, it was necessary to establish the functionality of the BPBio-hydrazide's crosslinking ability as well as its geometry. To establish this, four new probes were synthesized bearing a benzophenone and either a hydrazide, for site-specific linkage via ketone biotin, or an NHS ester, for linkage to surface-exposed lysine residues.

Benzophenone-NHS probes successfully produced dimer bands upon UV irradiation. By incubating p50 in the presence of 5 equivalents of BP-NHS or BP-Linker-NHS, a sufficient amount of benzophenone probe was loaded onto the protein surface to allow for photocrosslinking. This crosslinking was observed both in CFP controls as well as in p50. The crystal structures of GFP variants[22, 23] and p50[21] show a number of exposed lysine residues near the dimer interface. It is likely that the labeling of these positions is responsible for the formation of crosslinking products. This general surface labeling confirmed the presence of dimers under the assay conditions.

Benzophenone hydrazide probes were unable to produce dimer bands. Lack of hydrazide-ketone conjugation is unlikely to be a reason considering earlier labeling experiments as well as evidence that BP-hydrazide can compete away fluorescein-hydrazide labeling. The use of DNA bearing a p50 recognition site with or without added myotrophin, a protein known to induce the dimerization of p50 in the presence of DNA[19], failed to improve labeling.

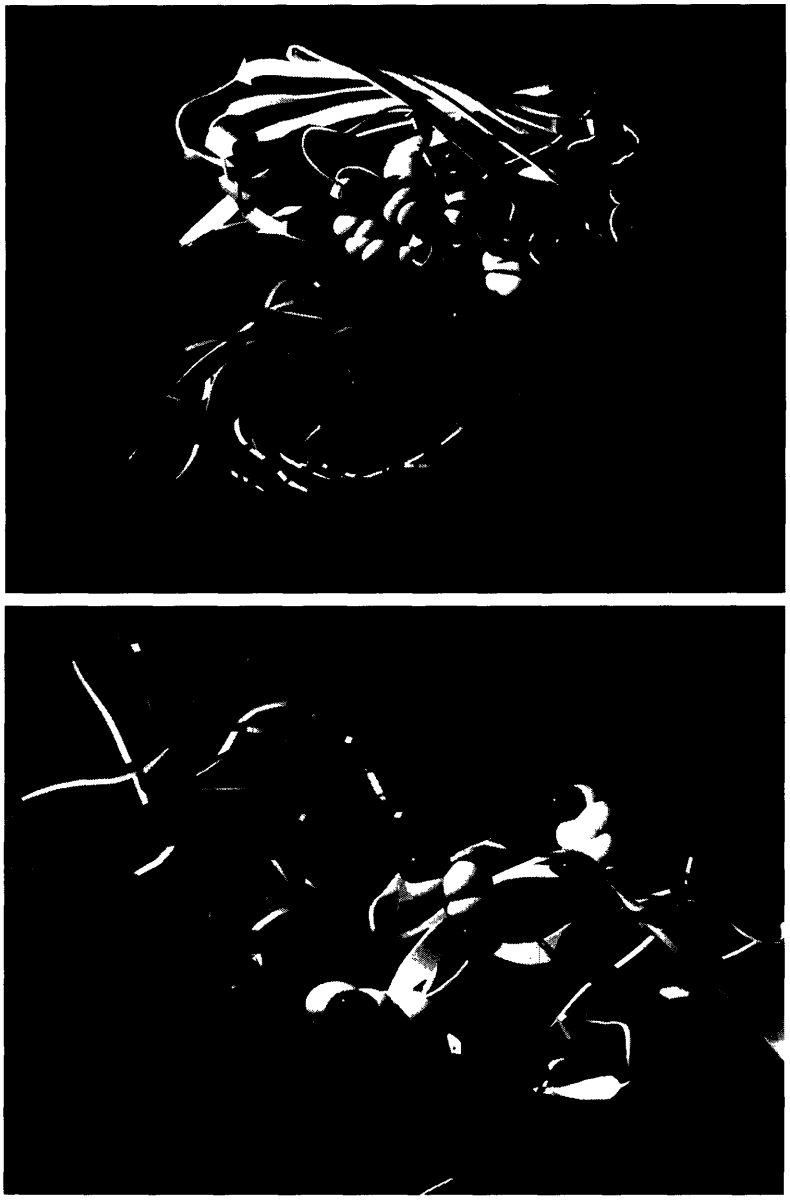

A

B

Figure 1-5: *Crystal structures of* ***A*** *GFP dimers*[23] *and* ***B*** *p50 dimer interface*[21]*. Side chains of lysine residues 41, 45, 209, and 214 in GFP and 272, 275, and 312 in p50 near the dimer interface are shown.*

The dimer bands noted by BP-hydrazide have also been found in the free benzophenone carboxylic acid, and are probably the product of hydrophobic interaction with the protein surface and multiple crosslinkings during UV irradiation. While benzophenone normally only forms one crosslink, the mechanism of photocrosslinking[24] does leave the possibility of multiple excitations and linkages if the phenyl radical performs the recombination instead of the carbonyl. Overall, none of the site-specific hydrazides could generate a satisfactory dimer band.

There are several possible reasons for the lack of site-specific crosslinking. One such reason is poor probe-protein geometry. Successful crosslinking events have been observed when using single, site-specific photophore labelings[25-28], so the number of photophores present is not likely an issue. However, their placement is quite critical. In all previous reports, the photophores responsible for generating the protein-protein linkages lie within close proximity to the interfaces between the proteins or between the protein and the nucleic acid. Furthermore, these photophores have very little mobility in their positions. Keeping the probe close to the interface and held in a rigid geometry to further encourage the interaction of the photo-activated probe are necessary for efficient crosslinkings. This is further demonstrated by the BP-NHS probes, which are incorporated near the dimer interface, and with little mobility compared to AP.

In our current design, the AP places the photophore on the end of a flexible peptide. As we lack data on the tertiary structure of the AP tag itself, it is possible that the photophore is too distant from the dimer interface to efficiently crosslink the proteins. The crystal structure does suggest that the AP tag may project over the p50 dimer interface towards the interacting partner, but the tag also contains a poly-glycine region that may give sufficient flexibility to the tag to move into a less productive orientation away from the interface.

Another possibility is that the extent of ketone biotinylation and hydrazide conjugation may be suboptimal. Its is not known at present if the current ketone biotinylation conditions allow for complete labeling of all AP-tagged proteins in the sample. If we assume hydrazide conjugation to be near complete, as the conditions used are quite forcing including both long conjugations times and large excess of hydrazide to ketone, the extent of ketone biotinylation will play a critical role in forming crosslinked products. Because both fluorescence (Figure 1-1B) and streptavidin-HRP detection (Figure 1-2B and C) are very sensitive, the observed signal may only represent a small fraction of the total protein content. The extent of ketone biotinylation combined with the considerations for the probe geometry relative to the dimer interface may reduce the crosslinking efficiency to near zero.

Both probe geometry and labeling extent will need to be modified to ensure good crosslinking efficiency. Movement of the AP tag from C- to N-terminal may bring the

photophore closer to the dimer interface in the case of CFP, but will not work for p50. The linker region between the AP and the protein could also be removed to bring the photophore in closer to the interface. While much more difficult, it may also be worthwhile to place the tag on an internal loop to force it to stay near the site of interaction. Optimization of KB labeling will require close analysis of the labeling extent followed by modifications of the time and concentrations of probe used to yield higher labeling.

Literature Cited

1. Phizicky, E. M.; Fields, S., Protein-Protein Interactions: Methods for Detection and Analysis. *Microbiol. Rev.* **1995,** 59, (1), 94-123.
2. Hell, S. W., Towards fluorescence nanoscopy. *Nature Biotechnology* **2003,** 21, (11), 1347-1355.
3. Lewis, A.; Taha, H.; Strinkovski, A.; Manevitch, A.; Khatchatouriants, A.; Dekhter, R.; Ammann, E., Near-field optics: from subwavelength illumination to nanometric shadowing. *Nature Biotechnology* **2003,** 21, (11), 1378-1386.
4. Robinson, J. M.; Takizawa, T.; Pombo, A.; Cook, P. R., Correlative Fluorescence and Electron Microscopy on Ultrathin Crossections: Bridging the Resolution Gap. *J. Histochem. and Cytochem.* **2001,** 49, (7), 803-808.
5. Cabantous, S.; Terwilliger, T. C.; Waldo, G. S., Protein tagging and detection with engineered self-assembling fragments of green fluorescent protein. *Nature Biotechnology* **2005,** 23, (1), 102-107.
6. Zal, T.; Gascoigne, N. R., using live FRET imaging to reveal protein-protein interactions during T cell activation. *Curr. Opinion in Immunology* **2004,** 16, 418-427.
7. Brock, R.; Hamelers, I. H. L.; Jovin, T. M., Comparison of Fixation Protocols for Adherent Cultured Cells Applied to a GFP Fusion Protein of the Epiderman Growth Factor Receptor. *Cytometry* **1999,** 35, 353-362.
8. Marks, K. M.; Rosinov, M.; Nolan, G. P., *In Vivo* Targeting of Organic Calcium Sensors via Genetically Selected Peptides. *Chem. Biol.* **2004,** 11, 347-356.
9. Guignet, E. G.; Hovius, R.; Vogel, H., Reversible site-selective labeling of membrane proteins in live cells. *Nature Biotechnology* **2004,** 22, (4), 440-444.
10. Adams, S. R.; Campbell, R. E.; Gross, L. A.; Martin, B. R.; Walkup, G. K.; Yao, Y.; Llopis, J.; Tsien, R. Y., New Biarsenical Ligands and Tetracystein Motifs for Protein Labeling *In Vitro* and *in Vivo*: Synthesis and Biological Applications. *J. Am. Chem. Soc.* **2002,** 124, 6063-6076.
11. Chen, I.; Howarth, M.; Lin, W.; Ting, A. Y., Site-specific labeling of cell surface proteins with biophysical probes using biotin ligase. *Nature Methods* **2005,** 2, (2), 99-104.
12. Kim, H.; Seo, J. Y.; Kim, K. H., NF-kB and Cytokines in pancreatic Acinar Cells. *J. Korean Med. Sci.* **2000,** 15, S53-S54.

13. Muller, C. W.; Harrison, S. C., The structure of the NF-kB p50:DNA complex: a starting point for analyzing the Rel family. *FEBS Letters* **1995,** 369, 113-117.
14. Udalova, I. A.; Richardson, A.; Denys, A.; Smith, C.; Ackerman, H.; Foxwell, B.; Kwiatkowski, D., Function Consequences of a Polymorphism Affecting NF-kB p50-p50 Binding to the TNF Promoter Region. *Molecular and Cellular Biology* **2000,** 20, (24), 9113-9119.
15. Ziegler-Heitbrock, L., The p50-homodimer mechanism in tolerance to LPS. *Journal of Endotoxin Research* **2001,** 7, (3), 219-222.
16. Bharti, A. C.; Aggarwal, B. B., Nuclear factor-kappa B and cancer: its role in prevention and therapy. *Biochemical Pharmacology* **2002,** 64, 883-888.
17. Beinke, S.; Ley, S. C., Functions of NF-κB1 and NF-κB2 in immune cell biology. *Biochem. J.* **2004,** 382, 393-409.
18. Huang, D.-B.; Vu, D.; Cassiday, L. A.; Zimmermanm, J. M.; Maher III, L. J.; Ghosh, G., Crystal Structure of NF-κB $(p50)_2$ complexed to a high-affinity RNA aptamer. *Proc. Natl. Acad. Sci.* **2003,** 100, (16), 9268-9273.
19. Knuefermann, P.; Chen, P.; Misra, A.; Shi, S.-P.; Abdellatif, M.; Sivasubramanian, N., Myotrophin/V-1, a Protein in the Failing Human Heart and in Postnatal Cerebellum, Converts NF-κB p50-p65 Heterodimers to p50-p50 and p65-p65 Homodimers. *J. Biol. Chem.* **2002,** 277, (26), 23888-23897.
20. Phelps, C. B.; Sengchanthalangsy, L. L.; Malek, S.; Ghosh, G., Mechanism of kB DNA binding by Rel/NF-kB dimers. *J. Biol. Chem.* **2000,** 275, (32), 24392-24399.
21. Sengchanthalangsy, L. L.; Datta, S.; Huang, D. B.; Anderson, E.; Braswell, E. H.; Ghosh, G., Characterization of the dimer interface of transcription factor NFkappaB p50 homodimer. *J Mol Biol* **1999,** 289, (4), 1029-40.
22. Rekas, A.; Alattia, J. R.; Nagai, T.; Miyawaki, A.; Ikura, M., Crystal structure of venus, a yellow fluorescent protein with improved maturation and reduced environmental sensitivity. *J Biol Chem* **2002,** 277, (52), 50573-8.
23. Yang, F.; Moss, L. G.; Phillips, G. N., Jr., The molecular structure of green fluorescent protein. *Nat Biotechnol* **1996,** 14, (10), 1246-51.
24. Dorman, G.; Prestwich, G. D., Benzophenone Photophores in Biochemistry. *Biochemistry* **1994,** 33, (19), 5661-5673.
25. Chavatte, L.; Frolova, L.; Kisselev, L.; Favre, A., The polypeptide chain release factor eRF1 specifically contacts the s(4)UGA stop codon located in the A site of eukaryotic ribosomes. *Eur J Biochem* **2001,** 268, (10), 2896-904.
26. Chen, M.; Samuelson, J. C.; Jiang, F.; Muller, M.; Kuhn, A.; Dalbey, R. E., Direct interaction of YidC with the Sec-independent Pf3 coat protein during its membrane protein insertion. *J Biol Chem* **2002,** 277, (10), 7670-5.
27. Chin, J. W.; Martin, A. B.; King, D. S.; Wang, L.; Schultz, P. G., Addition of a photocrosslinking amino acid to the genetic code of *Escherichia coli*. *Proc. Natl. Acad. Sci.* **2002,** 99, (17), 11020-11024.
28. Vidugiriene, J.; Vainauskas, S.; Johnson, A. E.; Menon, A. K., Endoplasmic reticulum proteins involved in glycosylphosphatidylinositol-anchor attachment: photocrosslinking studies in a cell-free system. *Eur J Biochem* **2001,** 268, (8), 2290-300.

Chapter 2: Design and synthesis of fluorescein phosphates for RNA selection

Introduction

Directed evolution methods have generated a variety of interesting and useful nucleic acid-based tools. Included among these are RNA aptamers, which are RNAs that adopt a secondary structure capable of selectively binding a target. Some of these take advantage of pre-existing nucleic acid affinities such as aptamers selected for binding to NF-κB p50[1], which mimic the structure of the DNA that p50 normally binds. Others are capable of binding entirely non-biological entities such as small molecule fluorophores[2-4]. The modulation the fluorescence intensity of these dyes upon binding[5] provides an avenue towards RNA-based detection systems. Appending a fluorophore-binding aptamer to an RNA would allow RNA tracking by fluorescence microscopy. This parallels a technique using small peptide tags that bind fluorophores that has already been demonstrated for protein tracking[6]. However, these methods lack any means of signal amplification as they can only bind a single dye molecule. This is important in cases where low copy numbers of the target are involved. Catalytic RNA species, known as ribozymes, allow such amplification to occur by allowing a single tagged RNA to process multiple dye molecules.

Like aptamers, a number of ribozymes with a variety of functions has been isolated from random sequence libraries. Again, these may mimic the activities found in natural ribozymes, such as phosphodiester transfer[7, 8], or perform more exotic roles including the catalysis of Diels-Alder reactions[9] and porphyrin metalation[10]. Allosterically regulated ribozymes are capable of detecting divalent metal ions[11] and microRNAs[12]. Ribozymes were particularly useful in the detection of miRNAs as they provided a much higher signal intensity and turn-on in the presence of their target versus conventional molecular beacons[12]. Whether selecting for a ribozyme or an aptamer, selection relies on the efficient separation of library members exhibiting the desired activity from the rest of the pool.

The use of immobilized substrates in a selection can allow for the separation of aptamer and ribozyme candidates from an RNA pool. Passing the library over a

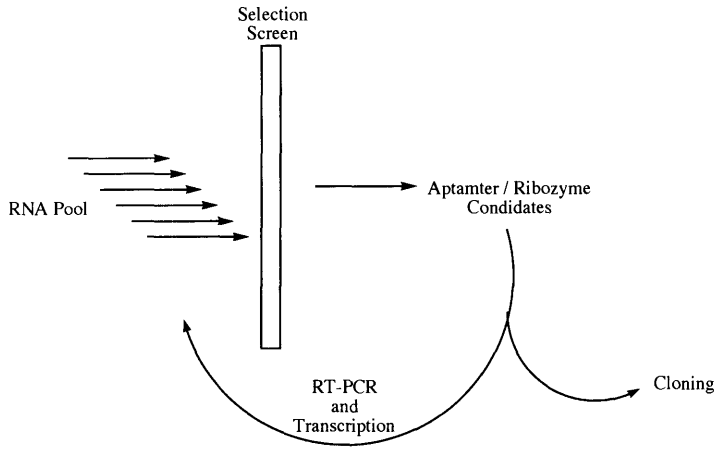

Figure 2-1: *Basic selection scheme used for aptamer and ribozyme selection. An RNA pool is screened against selection conditions, such as an immobilized substrate, to separate candidate sequences from the pool followed by amplification.*

column bearing the immobilized substrate allows the RNA to bind to the target, separating it from non-binding members that are washed away. Application of free substrate in solution can then compete for the RNA on the stationary phase carry it into solution for collection and amplification. Repeating iterative rounds of selection can yield an aptamer to the substrate. Modifying the selection conditions from a competitive elution to selection for probes capable of cleaving themselves from the solid phase allows for ribozyme selection[10]. However, the selection does not necessitate the use of an immobilized substrate.

In some cases, gel electrophoresis may separate ribozymes from the RNA pool. The selection of self-cleaving ribozymes is perhaps the simplest case. Cleavage results in fragmentation of the parent RNA, and these smaller segments can be separated by size in a gel, and thus isolated directly from the gel[13]. More subtle changes can be detected by modification of the gel conditions. The presence of an organomercurial agent, such as APM, within the gel selectively changes the mobility of thiol-containing compounds[14]. A ribozyme capable of catalyzing the formation of uridine from thiouracil and activated ribose was selected by isolating the RNA retarded by the incorporation of thiouracil in an APM gel[15]. RNA bearing a activated ribose at their terminus were exposed to thiouracil. Sequences capable of incorporating the thiouracil into their structure by forming thiouridine from their activated ribose were separated from the pool by APM-PAGE. Thus, these ribozymes were able to mimic the activity of uracil phosphoribosyltransferase, While thiouracil was used for this selection, reduced mobility in APM gels was originally found with thiophosphate monoesters[14].

Two sets of fluorescein-based probes were designed to use both immobilized and in-gel selection techniques. The first uses the immobilized substrate – competitive elution strategy to select for fluorescein phosphate aptamers and indirectly select for fluorescein phosphatase candidates. A fluorescein thiophosphate was also synthesized for the direct selection of a thiophosphatase using APM gels.

Results

A monomethyl fluorescein ether was synthesized for use in both phosphate syntheses as well later probes. 5(6)-carboxyfluorescein is readily formed from the condensation of resorcinol and trimellitic anhydride in methanesulfonic acid by adapting the methods of Hirano *et al*[16]. Precipitation from cold water and copious washing provided a nearly 1:1 mixture of regioisomers in near quantitative yield. Separation of these isomers was effected using the methods of Rossi and Kao[17]. The 6-carboxyfluorescein was then used for synthesis of the fluorescein methyl ether (6CFME) following the methods of Takakusa *et al*[18]. Improvement of yields in scale-ups of the 6-carboxyfluorescin dimethyl ester by up to 30% was possible by increasing the reflux time from overnight to 24 hours. Following methyl ether formation and methyl ester cleavage, the resulting fluorescein methyl ether was used in the synthesis of fluorescein phosphates, thiophosphates, and nucleoside-fluorescein conjugates. It was also possible to obtain the desired fluorescein methyl ether by treatment of carboxyfluorescein in the presence of excess base and methyl iodide followed by hydrolysis of the resulting methyl esters. However, a large excess of base is required to force the fluorescein out of the lactonized state to yield the monomethyl ether.

Both the fluorescein phosphate and fluorescein phosphate NHS ester were synthesized according to Takakusa *et al*[18] with some modifications (Scheme 2-1). 4,5-Dicyanoimidazole was found to be a good replacement for tetrazole as a phosphoramidite activator during phosphate synthesis. NHS ester formation was conducted as described in the literature, but deprotection of the phosphate by hydrogenation proved intractable. Under these conditions, the NHS ester was often

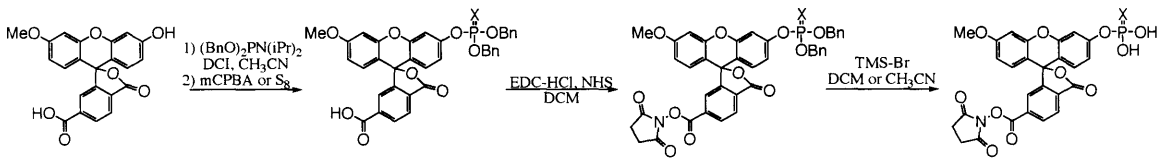

Scheme 2-1: *Synthesis of fluorescein methyl ether phosphate and thiophosphate NHS esters. a: X=O, b: X=S*

lost. However, the use of TMS-Br for deprotection[19] followed by HPLC purification led to the desired products.

Fluorescein diphosphate is a known substrate for alkaline phosphotase (CIP). 6CFME-phosphates should also be substrates, and thus an enzyme-based assay was used to verify the integrity of the products. 6CFME-phosphate was monitored for fluorescence in the presence and absence of CIP. A steady baseline was obtained in samples lacking the phosphatase, while a strong fluorescence signal rapidly developed in the presence of CIP (Figure 2-1). Satisfied with these results, a pair of solid phase resins for RNA selection were made.

Both 6-carboxyfluorescein and 6-carboxyfluorscein phosphate resins were produced from the NHS activated esters. 6-Carboxyfluorescein NHS ester was formed by reaction with N-hydroxysuccimide (NHS) and DCC in DMF. The dicyclohexyl urea was filtered off and the resulting NHS ester applied to 0.5 eq. Tentagel-HL-NH_2 resin. The 6CFME-phosphate resin was formed in a similar manner using the purified fluorescein phosphate NHS ester. Both resins were washed thoroughly to remove unbound material.

Next, an RNA library was needed for selection of a phosphate-selective aptamer. A region of 40 random nucleotides flanked by two different 15 nucleotide constant regions was chosen for this task. KpnI and Csp45I sites were included in the constant regions for cloning, and a T7 RNA polymerase promotor was used for *in vitro* transcription. The DNA template was synthesized by MWG Biotech, and used with a T7 Flash polymerase kit to form the library. The resulting RNA was purified on a PAGE-UREA gel, and the product band identified by UV-shadowing. The RNA was extracted from the gel using a crush-soak method on the excised band. The integrity of the RNA was confirmed by agarose gel as well as RT-PCR followed by cloning and sequencing.

Prior to selection, the initial library was assayed for phosphatase activity. Several commercial phosphate probes, including fluorescein diphosphate (FDP), DiFMUP, and DDAO phosphate, as well as 6CFME-phosphate were included in the screen. The probes were incubated at pH 8 in the presence of the RNA library and magnesium. In each case, a CIP-treated sample was included as a positive control. The initial library showed no phosphatase activity with any of the substrates even in the presence of magnesium. Whether this is due to the lack of a catalytic member in the library or simply low copy number could not be determined from this screening. However, the stability of the phosphates to the assay conditions was found to be satisfactory.

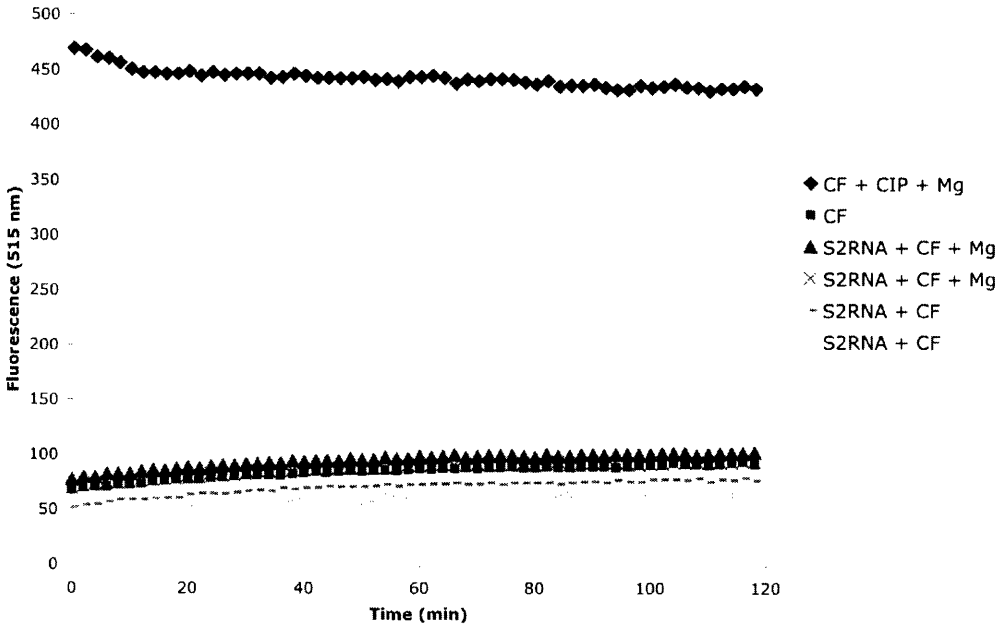

Figure 2-2: *Activity of RNA library towards fluorescein methyl ether phosphate (CF). No significant fluorescence increase is noted with RNA from the second selection round (S2RNA). Only treatment with alkaline phosphatase (CIP) produces a fluorescence increase. These data are representative of both the first round of selection and the initial library.*

With both the library and immobilized substrates in hand, several rounds of selection were attempted. Negative selection beads, bearing 6CFME, and positive

selection beads, loaded with the 6CFME-phosphate, were blocked for 20 minutes using 3% BSA in RNA binding buffer. The beads were washed twice with binding buffer prior to loading the RNA library. The library was then exposed to the negative selection beads for 15 minutes to eliminate non-specific binders. The negative selection beads were removed by centrifugation, and the supernatant was applied to positive selection beads. The RNA was allowed 30 minutes at 37 °C for binding. Unbound RNA was removed by washing the beads with 3% BSA and 0.1% Tween in binding buffer. Bound RNA was eluted from the beads using 100 μM 6CFME-phosphate. The resulting RNA was subjected to RT-PCR followed by cloning into pUC19 for sequencing.

The activity of the library was assayed after each of two round of selection. Exposure of the library to RNA from either round of selection to 6CFME-phosphate in the presence or absence of magnesium failed to show any catalytic activity (Figure 2-2). Sequencing data from the two rounds did not show any common sequence emerging. Further rounds of selection on a second library with these probes are being pursued.

A second selection system based upon fluorescein thiophosphate was also created. The synthesis of thiophosphate was initially conducted using a diethyl phosphate protection in place of dibenzyl. Chloro-diethylthiophosphate is commercially available, and reacts with 6CFME in the presence of NaH to give the corresponding thiophosphate. Attempts to deprotect this compound, however, were unsuccessful. Neither elevation of temperature nor changes in solvent or deprotection reagent were capable of removing the ethyl groups. A different approach was needed for the synthesis of the thiophosphofluoresceins.

The earlier phosphoramidite method for generation of the fluorescein phosphates was adapted to form the corresponding thiophosphates. Replacement of mCPBA with elemental sulfur under inert atmosphere formed the dibenzyl-protected thiophosphate. The rate of sulfurization is much slower than oxidation, but was accelerated by heating to 60 °C without damage to the compound. Purification by silica column met with mixed results, and was replaced by purification by reverse-phase semi-preparative HPLC. Formation of the NHS ester was accomplished by standard carbodiimide chemistry.

TMS-Br was again used to deprotect the thiophosphate. Cleavage of the benzyl groups in either dry acetonitrile or dichloromethane at ambient temperature resulted in

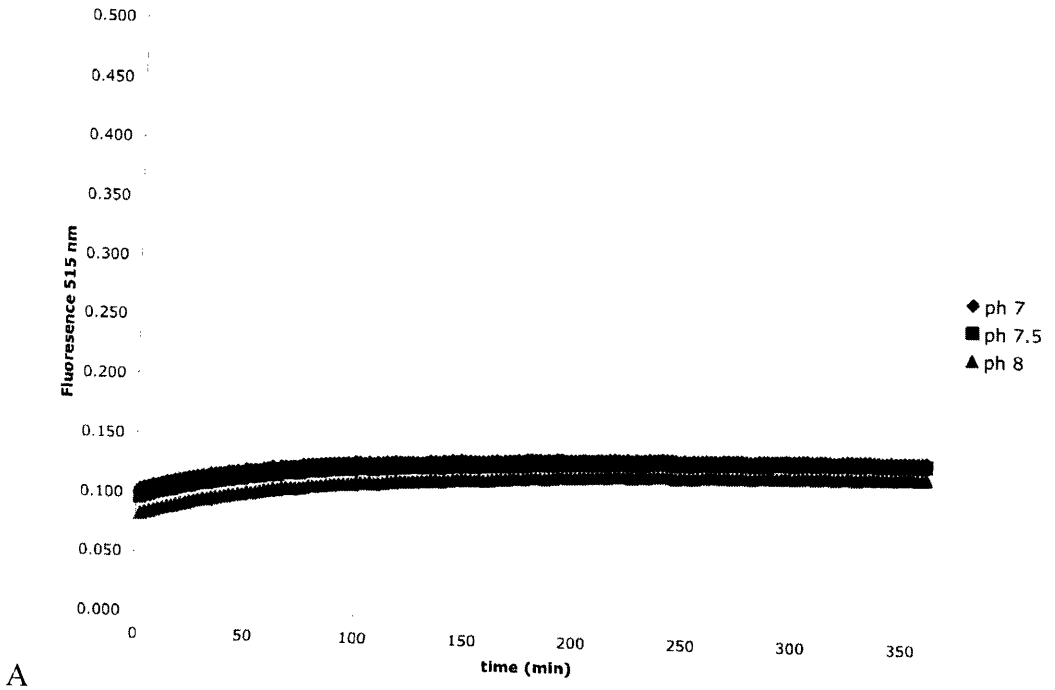

A

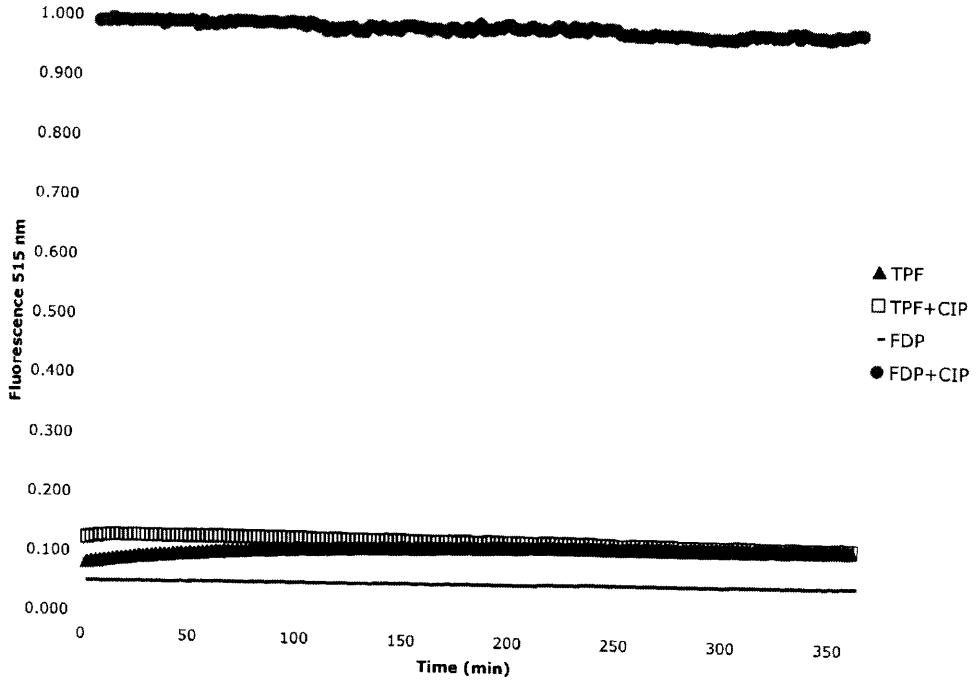

B

Figure 2-3: A: *pH stability profile of fluorescein thiophosphates monitored at 2 min intervals. Fluorescence is normalized to 1 corresponding to the turn on of an equal concentration of FDP treated with CIP.* ***B:*** *Stability of thiophosphate in the presence of alkaline phosphatase (CIP) at pH 8.*

cleavage of only one benzyl group. Reactions conducted at 55 °C in acetonitrile, however, resulted in a mixture of products corresponding to the loss of either one or both benzyl groups. These compounds were readily separated by reverse- phase HPLC to provide the final product. Combined with N-acryloyl-p-aminophenylmercuric acetate (APM), synthesized according the literature methods[14], the thiophoshates are being used for selection of a fluorescein thiophosphatase.

In preparation for use in-gel, two aspects of the thiophosphate were examined. First, the stability of the thiophosphate at variable pH was assessed to address concerns of degradation during DNA coupling or in the gel. Three pH values, used for either coupling or are present in the gel, were examined. All three show a slow drift towards higher fluorescence, but none of these values approaches the full fluorescence turn-on (Figure 2-3A). Second, the stability of these compounds in the presence of alkaline phosphatase was tested. No significant change was observed between phosphatase treated samples and negative controls. The observed fluorescence was far below that of phosphatase-treated FDP of equal concentration included as a positive control (Figure 2-3B).

Figure 2-4: *APM-PAGE gel of TPF-labeled DNA.* ***A*** *TPF conjugated to DNA,* ***B*** *CFME conjugated to DNA,* ***C*** *DNA only,* ***D*** *TPF-conjugated DNA after NaOH treatement. DNA was* ^{32}P *–end labeled for detection on a phosphor screen. Image courtesy of Dr. D. Chinnapen, used with permission*

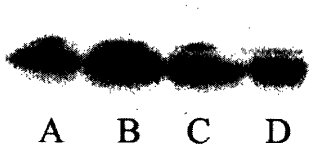

Thiophosphofluorescein NHS ester (TPF) reduces the mobility of amine-labeled DNA. An excess of a small DNA splint bearing a terminal amine was reacted with TPF in carbonate buffer at pH 8. TPF-labeled DNA could be separated from unlabeled DNA in a 16% polyacrylamide gel containing 80 μM APM (figure 2-4). The addition of the non-thiophosphorylated fluorescein had identical mobility to the DNA alone. Thus, APM-PAGE can successfully separate thiophorphorylated and non-thiophosphoyrlated fluorescein-nucleic acid conjugates, and may be used for the selection of a thiophosphatase ribozyme.

Discussion

Both fluorescein and phosphofluorescein required for aptamer selection were successfully synthesized and immobilized on Tentagel resin. Furthermore, initial selection rounds have been conducted using this resin pair. While these rounds did not yield a consensus sequence or catalytic species, this is not entirely surprising. As this pair of resins is better suited to aptamer selection, the chances of finding a catalytic species within it without further selective pressure are rather low. However, both the use and recovery of RNA from the beads demonstrates the potential of the system for selection of a phosphate-specific aptamer. New libraries and modified selection procedures that monitor for both binding and catalytic activity are being conducted with these resins.

Thiophoshate analogues of the resin-bound probes allows for the more direct selection of a catalytic species. These compounds have demonstrated stability at physiological pH as well as resistance to phosphatase treatment. While alkaline phosphatase was unable to cleave the thiophosphate under the assay conditions, it is likely that a ribozyme can be selected that is capable of this task. As alkaline phosphatase cannot cleave this thiophosphate efficiently, it is possible that other phosphatases will show poor activity towards this substrate, which is desirable when trying to limit background hydrolysis in cell-based assays.

The thiophosphate NHS esters have been conjugated to amino-linked DNA splints for use in ribozyme selection. The activated esters have been distributed within the lab for further testing and ribozyme selection. Recent results from this work have shown that

^{32}P end-labeled oligonucleotides bearing an primary amine linker are retarded on APM-PAGE in a thiophosphate-dependant manner. Isolation and ligation of this splint DNA to an RNA library will allow for the selection of thiophosphatase ribozymes. As both the thiophosphate monoester and diester are available from this synthesis, it may also be interesting to confirm that the conclusions of Igloi[14] concerning the complexation of thiophosphates to mercury in-gel holds for a less sterically hindered aryl thiophosphate.

Literature Cited

1. Ghosh, G.; Huang, D.-B.; Huxford, T., Molecular mimicry of the NF-kB DNA target site by a selected RNA aptamer. *Curr. Opinion in Struct. Biol.* **2004,** 14, 21-27.
2. Baugh, C.; Grate, D.; Wilson, C., 2.8 A crystal structure of the malachite green aptamer. *J Mol Biol* **2000,** 301, (1), 117-28.
3. Holeman, L. A.; Robinson, S. L.; Szostak, J. W.; Wilson, C., Isolation and characterization of fluorophore-binding RNA aptamers. *Fold Des* **1998,** 3, (6), 423-31.
4. Nguyen, D. H.; DeFina, S. C.; Fink, W. H.; Dieckmann, T., Binding to an RNA aptamer changes the charge distribution and conformation of malachite green. *J Am Chem Soc* **2002,** 124, (50), 15081-4.
5. Babendure, J. R.; Adams, S. R.; Tsien, R. Y., Aptamers switch on fluorescence of triphenylmethane dyes. *J Am Chem Soc* **2003,** 125, (48), 14716-7.
6. Marks, K. M.; Rosinov, M.; Nolan, G. P., *In Vivo* Targeting of Organic Calcium Sensors via Genetically Selected Peptides. *Chem. Biol.* **2004,** 11, 347-356.
7. Ikeda, Y.; Taira, K., Biologically Important Reactions Catalyzed by RNA Molecules. *The Chemical Record* **2002,** 2, 307-318.
8. Puerta-Fernandez, E.; Romero-Lopez, C.; Barroso-delJesus, A.; Berzal-Herranz, A., Ribozymes: recent advances in the development of RNA tools. *FEMS Microbiol Rev* **2003,** 27, (1), 75-97.
9. Serganov, A.; Keiper, S.; Malinina, L.; Tereshko, V.; Skripkin, E.; Hobartner, C.; Polonskaia, A.; Phan, A. T.; Wombacher, R.; Micura, R.; Dauter, Z.; Jaschke, A.; Patel, D. J., Structural basis for Diels-Alder ribozyme-catalyzed carbon-carbon bond formation. *Nat Struct Mol Biol* **2005,** 12, (3), 218.
10. Breaker, R. R., *In Vitro* Selection of Catalytic Polynucleotides. *Chem. Rev.* **1997,** 97, 371-390.
11. Zivarts, M.; Liu, Y.; Breaker, R. R., Engineered allosteric ribozymes that respond to specific divalent metal ions. *Nucleic Acids Research* **2005,** 33, (2), 622-631.
12. Hartig, J. S.; Grune, I.; Najafi-Shoushtari, S. H.; Famulok, M., Sequence-Specific Detection of MicroRNAs by Singal-Amplifying Ribozymes. *J. Am. Chem. Soc.* **2004,** 126, 722-723.
13. Roth, A.; Breaker, R. R., Selection In Vitro of Allosteric Ribozymes. *Methods in Molecular Biology* **2004,** 252, 145-164.

14. Igloi, G. L., Interaction of tRNAs and of Phosphorthioate-Substituted Nucleic Acids with an Organomercurial. Probing the Chemical Environment of Thiolated Residues by Affinity Electrophoresis. *Biochemistry* **1988,** 27, 3842-3849.
15. Urau, P. J.; Bartel, D. P., RNA-catalysed nucleotide synthesis. *Nature* **1998,** 395, 260-263.
16. Hirano, T.; Kikuchi, K.; Urano, Y.; Nagano, T., Improvement and biological applications of fluorescent probes for zinc, ZnAFs. *J Am Chem Soc* **2002,** 124, (23), 6555-62.
17. Rossi, F. M.; Kao, J. P. Y., Practical Method for the Multigram Separation of the 5- and 6-Isomers of Carboxyfluorescein. *Bioconj. Chem.* **1997,** 8, 495-497.
18. Takakusa, H.; Kikuchi, K.; Urano, Y.; Kojima, H.; Nagano, T., A Novel Design Method of Ratiometric Fluorescence Probes Based on Fluorescence Resonance Energy Transfer Switching by Spectral Overlap Integral. *Chem Eur. J.* **2003,** 9, (7), 1479-1485.
19. Lazar, S.; Guillaumet, G., A selective removal of benzyl protecting groups in arylphosphate esters with bromotrimethylsilane. *Synthetic Communications* **1992,** 22, (6), 923-931.

Chapter 3: Design and synthesis of nucleoside-based fluorogenic probes for RNA selection

Introduction

A healthy cell must produce a plethora of proteins at the right time as well as in the right place. Improper timing or localization could lead to impairment of function or cell death. Nature has constructed a complicated network of interactions to ensure the proper correlation of protein expression with both the cell cycle and external stimuli. Likewise, the cell has an array of methods to ensure that those proteins, once expressed, reach their proper destination.

One method to properly target proteins to a specific location within a cell involves the use of signaling sequences. These sequences are recognized by other components of the cell for transport or for post-translational modification to assist in delivery. Examples of such signals include nuclear localization sequences[1, 2] and the CAAX motif found in $p21^{Ras}$ that signals for farnesylation necessary for membrane localization[3-5]. However, such tags are not the only method available for the control of protein localization.

Localization of mRNA transcripts also provides spatial control of protein expression. Transportation of mRNA to specific sites within the cell allows for expression of the encoded protein where it is needed. Localization of mRNA is a significant phenomenon during development. Among the best-studied examples of these are *bicoid* and *nanos* transcripts in *Drosophila* oocytes. These transcripts encode proteins responsible for differentiation of posterior and anterior body plans, and are localized to opposite poles of the oocyte[6, 7]. Many localized transcripts have also been found important in the development in *Xenopus* oocytes[7]. Improper localization of these transcripts would lead to disruption of normal development. The importance of RNA localization is, however, not limited to that observed in development.

Localization of mRNA's within neurons has been observed in both dendrites and axons. Transcripts localized to the axon include, but are not limited to, those of vasopressin and oxytocin in mammals and neurofilament proteins in squid giant axons[8]. Localization of myelin transcripts to distal portions of oligodendrocytes has been

implicated in the delivery of myelin proteins[9]. A number of RNAs appear at dendritic sites along with synapse associated polyribosome complexes for their translation[6, 10]. Detection of these transcripts, however, has many limitations.

Perhaps the most sensitive means of RNA detection is PCR. As PCR confers amplification of the transcripts, detection of targets present in low copy number is possible. Amplification of dendritic or axonal transcripts, however, is not simple. RNA from these cellular processes must be collected without contamination from the soma or from neighboring neurons or glia. Collection of the RNA also disrupts the cellular structure, causing loss of spatial and temporal information. While very sensitive, PCR cannot provide sufficient spatial or temporal information. *In situ* hybridization, however, can provide a better image of RNA localization.

In situ hybridization is a method of saturation binding followed by excess probe removal. A set of cells is first fixed, then permeablized to allow probe entry. An excess of labeling reagent, complimentary to the RNA to be studied, is added and the excess washed away. The localization of the probe can then be studied using microscopy as in the case of fluorescence *in situ* hybridization. While this provides a more precise location of RNA transcripts, it requires fixation of the cell and thus loss of temporal information in RNA trafficking. An *in vivo* imaging agent would allow for the preservation of both spatial and temporal data.

Molecular beacons allow imaging of RNA localization *in vivo*. These probes consist of nucleic acid sequences with a fluorophore and a quencher attached at opposite ends. When isolated, the beacons have a stem-loop conformation that places quencher and fluorophore in close proximity. When the probe hybridizes with its target RNA sequence, the quencher and fluorophore are separated, resulting in a fluorescent signal. While these probes are quite versatile, they suffer from several drawbacks.

Background fluorescence due to nuclease activity, difficulty in probe delivery, and lack of signal amplification are common problems experienced when using molecular beacons. DNA and RNA based molecular beacons are degraded by their respective nucleases, resulting in false positives. Solutions to these problems include the use of 2'O methyl ribonucleotides to confer nuclease resistance[11] or molecular beacon FRET pairs[12]. These probes, however, still require microinjection, making their use on

large cell populations difficult. Molecular beacon delivery by fusion to TAT peptide appears to be a feasible solution to these delivery issues[13]. While these efforts have made the use of molecular beacons more feasible, they still may not be able to detect mRNAs present in very low numbers as they lack any form of signal amplification. A new *in vivo* imaging system would be able to confer the spatial and temporal resolution of molecular probes with sensitivity enhancement by signal amplification. Ribozymes provide an attractive route to such a target.

Ribozymes are RNA species with catalytic activity. While they vary in size and secondary structure, they typically catalyze the cleavage and formation of phosphodiester bonds. Ribozymes are not limited to these reactions, as has been demonstrated by ribozymes that catalyze Diels-Alder reactions[14]. Another example selected for by *in vitro* evolution methods includes ribozymes capable of nucleotide synthesis[15]. Appending a ribozyme to an RNA would allow for a genetically encoded RNA tracking device. Its catalytic activity could provide signal amplification detectable by fluorescence microscopy when provided with a matching fluorogenic substrate. With the proper selection criteria, the selection of such a ribozyme is possible.

Selection of a ribozyme requires a means of separating catalytic targets from inactive members of a library. Immobilization of the substrate on a solid phase support allows for the exclusion of non-binding RNA's in the library. By anchoring the solid phase to one end of the substrate and the ribozyme binding position to the other, catalytic RNA that cleaves the probe in half can be collected after application of selection conditions, such as the addition of magnesium, by rinsing the resin and collecting the filtrate. Amplification of this pool by PCR provides a new library for further rounds of selection. The use of this strategy, however, requires the synthesis of an appropriate immobilized substrate.

A nucleoside-fluorescein conjugate was chosen as the substrate for the ribozyme. The dye bears a fluorophore attached to a nucleoside in a manner similar to RNA. Upon recognition, the ribozyme, which will be fused to a target RNA, will catalyze the formation of a 2'O-3'O cyclic phosphate with release of the fluorophore (Figure 3-1). Thus, the tracked RNA will generate a fluorescent signal in the presence of the dye substrate that can be monitored by fluorescence microscopy.

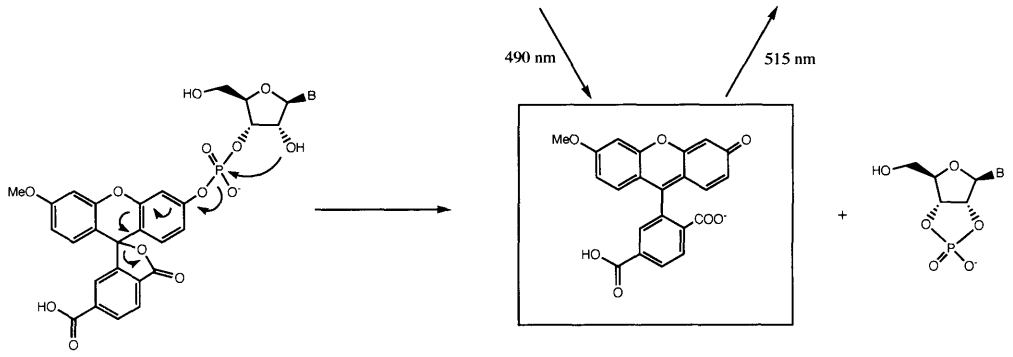

Figure 3-1: *Mechanism of ribozyme-catalyzed release of fluorophore and generation of fluorescent signal*

Results

Selective protection of the 5' and 3' hydroxyl groups was achieved by use of TIPDS-Cl_2[16]. Treatment with 1.1 eq of the disilyl reagent in pyridine gave the protected nucleosides in nearly quantitative yield. Masking of the adenosine N^6 amino group was also necessary. Pre-treatment with TMS-Cl to temporarily block the 2' hydroxyl followed by the addition of Bz-Cl and subsequent NH_4OH treatment provided the mono-benzoylated adduct[17]. The product was also obtained by treatment with excess Bz-Cl to give the 2'O, N^6, N^6-tribenzoylated intermediate. Sodium methoxide in ethanol on ice for 15-30 minutes then provided the N^6-benzoylated product[16]. From this product, protection of the 2' position and exposure of the 3' for fluorescein coupling could proceed.

Two variants on the acid-labile 2'O protection with 5'O silyl protection were synthesized. Neat ACE orthoester in the presence of PPTS at elevated temperatures under vacuum followed by TEA / HF treatment generated the 2'O-ACE protected compound with free 3'O and 5'O sites in modest yield[18]. The use of ACE for 2' protection was later replaced by THP as it was more readily available, could be installed in quantitative yield in the presence of catalytic TsOH, and was stable to TEA / HF cleavage conditions to provide the 2'O protected adduct in higher yield. For both compounds, we relied on the preference of the TBDMS group for the primary hydroxyl to give the 5'O-TBDMS adducts which were then ready for use in phosphoramidite chemistry.

Generation of the fluorescein – nucleoside phosphate junction required two stages. First, the 3' hydroxyl is converted to the phosphoramidite by reaction with $(iPr_2N)_2POMe$ in the presence of 4,5-dicyanoimidazole (DCI) as an activator. Anhydrous conditions under inert atmosphere are necessary at this stage to prevent oxidation or the

formation of the phosphite. The nucleoside phosphoramidite was separated from excess phosphordiamidite by silica chromatography followed by drying under vacuum. 6-Carboxyfluorescein methyl ether (6CFME) and 4-5 dicyanoimidazole (DCI) were then added and the atmosphere replaced with argon. Coupling proceeded in dry acetonitrile at ambient temperature, generally reaching completion within 30 minutes. Complete consumption of the phosphoramidite and the presence of the phosphite intermediate were observed by ESI-MS in positive ion mode. Oxidation of this intermediate to the phosphate proceeded smoothly upon addition of excess mCPBA.

Purification of the nucleoside-fluorescein phosphate triester proved problematic. Pure samples of the ACE and THP protected compounds could not be isolated from silica columns under a multitude of conditions. Before the availability of an easily accessed ESI-MS, the reactions were thought to have failed entirely. Commercial 2'O-ACE, 5'O-silyl protected 3'O adenosine phosphoramidite was purchased from Dharmacon to troubleshoot the reactions without success until LC/MS was available for analysis. Purification of the commercial adenosine probe, as well as the THP-protected compound, was then completed on a reverse phase column.

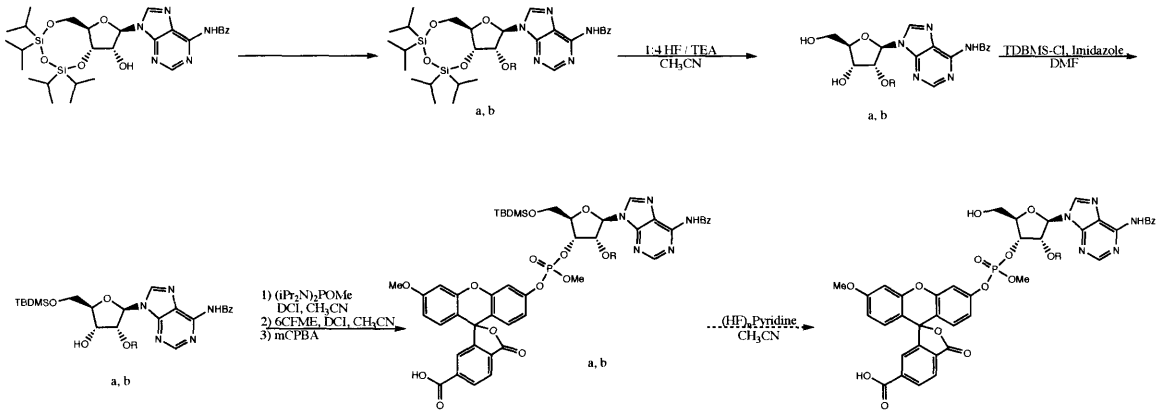

Scheme 3-1: *Synthesis of acid-labile 2'O protected 3'O-fluorescein phosphates. A: R=ACE, B: R=THP*

Two additional adenosine-based probes were synthesized from intermediates in the acid-labile 2'O strategy. The first of these uses the tribenzoylated intermediate isolated during the benzoyl protection of the adenosine N^6 position. The 3'O, 5'O- silyl deprotection was cleaved in the presence of TEA / HF, and the 5'O-TBDMS protection installed as previously described. Application of the same two-stage phosphate formation

yielded the adenosine-fluorescein conjugate. The second derivative replaces the 2'O protection step with the phosphate linkage to the fluorescein to provide a 2'O fluorescein phosphate with 3'O-5'O-TIPDS protection.

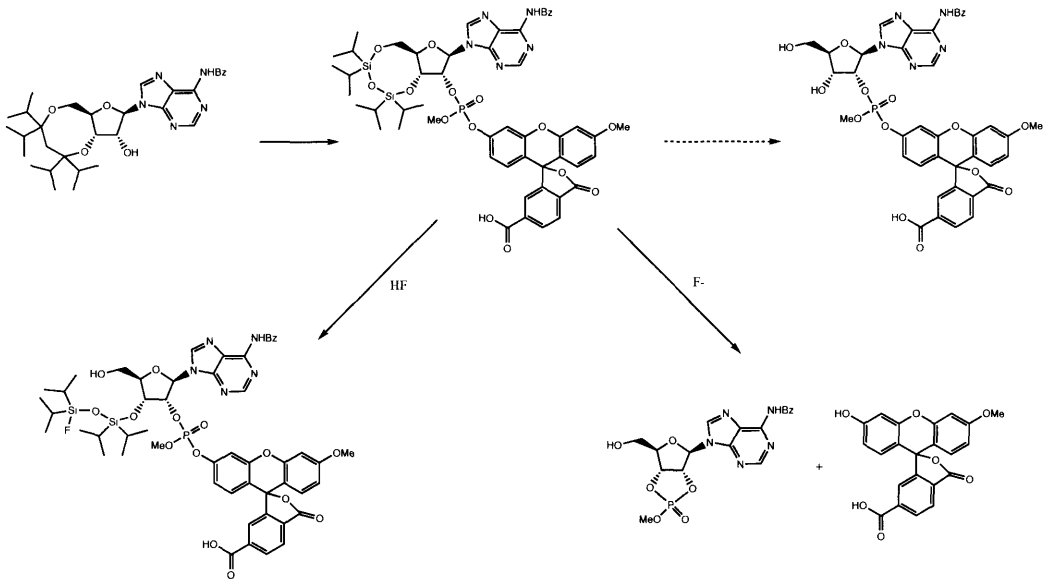

Scheme 3-2: *2'O-fluorescein phosphate synthetic strategy and observed side products*

In preparation for loading onto the silyl resin, the 5'O protecting groups were removed. The standard TIPDS removal conditions using TEA / HF were unsuitable for the 2'O phosphate as the basic conditions caused the free 3' hydroxyl to attack the phosphate and form the cyclic AMP ester with loss of fluorescein. Removal of TEA from the system to provide more acidic conditions still failed to prevent cyclization, and only a partial fluoridolysis product could be isolated. Thus, the 2'O phosphate strategy was abandoned. Removal of the 5'O TBDMS from the tribenzoyl derivative proceeded smoothly in the presence of dilute HF. Fluoridolysis of the silyl groups in both ACE and THP derivatives gave very low yield over a variety of conditions as indicated by LC/MS and from purified reactions.

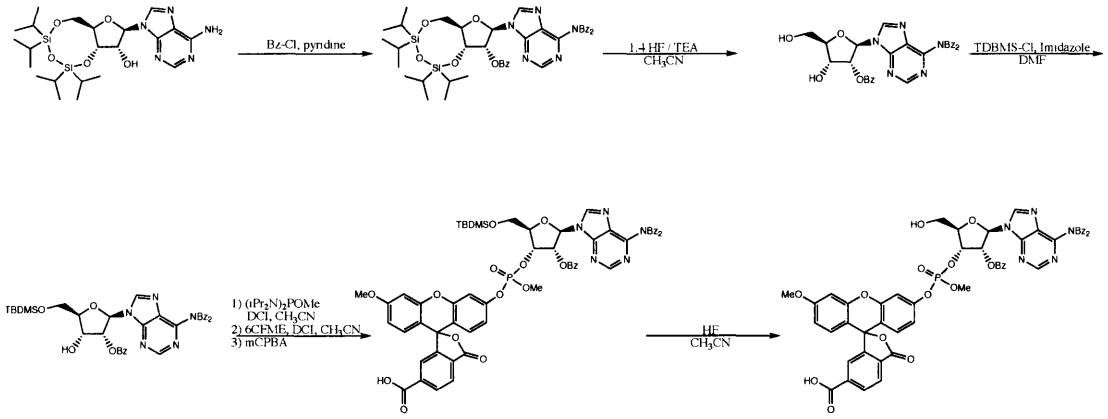

Scheme 3-3: *Synthesis of tribenzoyl adenosine fluorescein phosphate before solid phase loading*

Before attempting resin loading, the deprotection steps to follow while on solid phase were tested in solution. The first of these is removal of the phosphate methoxy protection to yield the phosphate diester. Treatment with a 1 M solution of disodium-2-carbamoyl-2-cyanoethylene-1,1-dithiolate trihydrate (S2Na2) in DMF for 1 hour gave complete conversion to the phosphate diester, which could be purified by reverse phase HPLC. Several attempts to remove the acetyl groups of ACE or the 2'O-benzoyl protection on the tribenzoyl-adenosine with primary amines suffered from the same cyclization event observed in the 2'O-fluorescein phosphate method. Efforts were then focused on the 2'O-THP strategy to make the final probe suitable for solid phase use.

The 5'O-TBDMS and 3'O-THP deprotections were closely examined by a combination of ESI-MS and LC/MS. TBDMS cleavage was tested under a variety of fluorine sources including varied concentrations of HF, TEA / HF, pyridine / HF, and TBAF. Removal of THP was attempted under acidic conditions as well as under neutral conditions with Lewis acid catalysts[19, 20]. All buffered fluorine sources were capable of cleaving the TBDMS group without displacement of the THP. Unfortunately, it was discovered that fluoridolysis of the phosphate triester to form a fluorophosphate with release of fluorescein was far more facile than removal of TBDMS. Unbuffered HF was capable of removing the TBDMS group with a significant loss of THP as well. Non-specific cleavage of both TBDMS and THP were noted in most acid-promoted cleavages for THP despite some cases of selectivity found in the literature. The use of Lewis acid-promoted cleavage under neutral conditions, also known to be selective for THP over

TBDMS, was incompatible with the phosphate as both the triester and diester were rapidly converted to cyclic AMP esters with loss of fluorescein.

An orthogonal approach to the fluorescein-nucleoside probe was necessary as the current strategy was incompatible with the sensitive β-hydroxyl aryl phosphate. A 5'O-dimethoxytrityl (DMTr) and 2'O-p-methoxybenzyl (PMB) system was chosen to replace the earlier system. Direct incorporation of PMB to the 2'O position of 5'O-3'O TIPDS protected adenosine or uridine was found to be difficult due steric crowding at the site. Benzylation of the nucleobase was more prominent under the conditions examined. The use of a 2'O-3'O-(dibutylstannylene)-uridine[21] was chosen as an alternative route. Reaction of the tin complex with PMB-Cl at 110 °C in dry DMF yielded a mixture of 2'O and 3'O-PMB uridines. The 5'OH was then selectively protected using DMTr-Cl in pyridine[21].

Conjugation of the fluorescein-uridine conjugate and 5' deprotection was examined next. The earlier strategy of phosphoramidite formation followed by fluorescein addition and oxidation yielded the desired product without the need for any further protection of the uridine. Removal of the DMTr group from the crude mixture was observed using 1.5% TsOH in 10% (v/v) MeOH / DCM at ambient temperature, and the product verified by ESI/MS/MS.

Discussion

Several routes and model compounds have resulted from the efforts to generate a solid-phase selection probe. These models allowed for insight into the reactivity of the aryl phosphate triester and considerations that must be made in attempting to immobilize this target. The acid-catalyzed deprotection and nucleophilic deprotection models contributed to this knowledge in their own ways.

From the nucleophilic deprotection models, the stability of the aryl phosphate triester was assessed during 5'OH deprotection. As these model compounds used silyl protection in both cases, fluoridolysis was chosen for their removal. The TBDMS group in the 2'O-benzoyl protected model was readily removed in dilute hydrofluoric acid in acetonitrile without formation of the cyclic phosphate or loss of the 2'O protection. 5'O-

3'O-TIPDS protection, however, was not successfully removed under these conditions. Even without a basic buffering agent, the phosphate triester was attacked by the exposed 3'OH to yield the cyclic phosphate with loss of fluorescein. Likewise, the phosphate triester could not be exposed to the 2'OH during hydrolysis of the benzoyl ester without cyclization occurring. Thus from these models, the necessity of a non-nucleophilic cleavage of the neighboring protecting group will be necessary for successful probe synthesis.

As nucleophilic cleavages of the protecting groups cannot yield a stable product, acid-catalyzed deprotection was examined, and made to mimic the current RNA synthesis procedures. Both the ACE protecting group (Dharmacon) and the tetrahydropyranyl (THP) were examined as 2'O protecting agents. In both cases, 5'O silyl protection was used. Both compounds could be incorporated at the 2' position under mild acidic conditions. Removal of the TIPDS protection followed by selective protection of the primary hydroxyl allowed for a 3'O fluorescein phosphate to be synthesized. Before these probes could be loaded onto solid phase, the 5'O silyl protection needed to be removed. The use of TEA / HF as in commercial synthesis was found to be unsatisfactory with this system. Unlike the alkyl phosphate triesters, the fluorescein phosphate triester was readily cleaved by the basic fluoride ion to release fluorescein. Several attempts to decrease the nucleophilicity of the fluoride ion by increasing the ratio of HF to buffering agents such as triethylamine and pyridine failed to improve the situation. Only in the presence of dilute HF was 5'O deprotection successful. However, this also yielded loss of the ACE and THP groups as indicated by LC/MS. It should be noted that the phosphate diester, lacking the methyl protection, is stable to TEA /HF treatment at ambient temperature. While this series of probes cannot provide the selectivity for 5' versus 2' deprotection needed on the silyl resin, it does offer a viable route to the solution-phase synthesis of the free dye that will be needed for later experiments. Solid-phase probes, however, will require an alternative route.

Based on the knowledge gained from the earlier synthetic routes, the 4-methoxybenzyl (PMB) group was chosen for the protection of the 2'OH. The PMB group is stable to acidic conditions allowing for the use of TsOH treatment for 5'OH deprotection. Unlike the benzoyl and acid-labile protecting groups, PMB can be cleaved

oxidatively in the presence of DDQ in water / dichloromethane. PMB is also cleaved at a much higher rate than an unmodified benzyl group, allowing for more rapid deprotection without damage to the resin itself. Furthermore, DDQ has been used in the presence phosphates for deprotection[22] and should leave the phosphate diester untouched.

Use of the TIPDS-protected nucleosides proved difficult for 2'O PMB protection. Several attempts under a variety of conditions including variations in the base used, temperature, solvent, concentration, and the presence of catalysts such as TBAI failed to produce the 2'O protected product. While there are a few examples of this protection in the literature, the replication of these strategies was unsuccessful with PMB-Cl. To circumvent this problem, 2'O-3'O-(dibutylstannylene)-uridine was synthesized[21]. Treatment of this complex at 110 °C in dry DMF successfully generated a mixture of 2'O and 3'O PMB uridines in modest yield. These compounds could then be 5'O protected with either TBDMS or DMTr to give either an open 2'O or 3'O position for fluorescein phosphate formation.

Coupling of the fluorescein to these analogs to proceeded in a similar manner as the four model compounds presented earlier. It may also be possible to purify these compounds in a manner similar to that of the 2'O-benzoyl model, provided the compound proves to be stable on silica. However, reverse-phase purification is recommended to ensure complete removal of excess fluorescein. Detritylation of the 5'OH is possible with TsOH. The 5'OH deprotected compound is then ready for solid phase loading.

To finish the probe, a few modifications must be conducted on solid phase (Scheme 3-4). Once the probe is bound to the solid phase, the carboxylic acid of fluorescein is activated using a carbodiimide such as EDC-HCl in the presence of N-hydroxysuccinimide to form the activated ester. Excess EDC must be washed away afterwards to prevent it from activated the phosphate groups of the amine-bearing DNA oligonucleotide that is added next. Similarly, the fluorescein phosphate must not be deprotected until the DNA has been coupled to the probe. Treatment of this resin with S_2Na_2 (Dharmacon) in DMF will then yield the deprotected phosphate. The final step in the probe synthesis is the treatment of the resin with aq. DDQ in dichloromethane. This removes the PMB group and leaves the fully deprotected probe bound to the resin.

The resin can then be treated with the RNA library bearing a constant region complimentary to the DNA oligo located on the resin. Once the library is bound to the probe on the resin, the conditions for cleavage can be made permissive by the addition of magnesium to the buffer. Any ribozyme capable of cleaving the cleaving the phosphate bond at that point will sever itself from the resin for recover and amplification by RT-PCR. Repeated iterative rounds of selection should then yield a species with the desired catalytic activity.

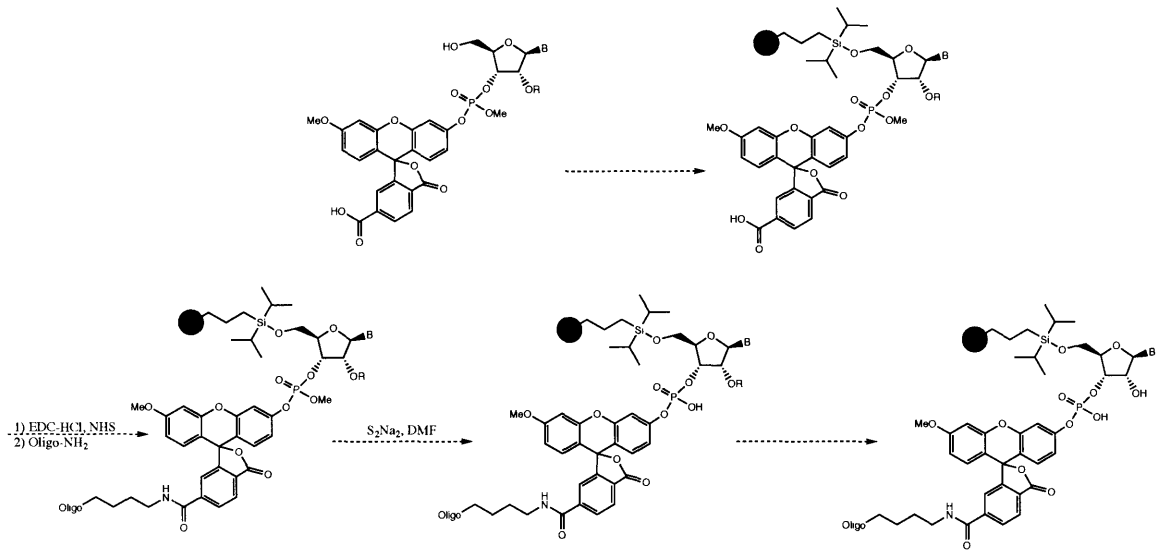

Scheme 3-4: *General loading procedure and deprotection for solid phase selection probe*

Literature Cited

1. Izaurralde, E.; Adam, S., Transport of macromolecules between the nucleus and the cytoplasm. *RNA* **1998,** 4, 351-364.
2. Maraia, R. J., La Protein and the Trafficking of Nascent RNA Polymerase III Transcripts. *J. Biol. Chem.* **2001,** 153, F13-F17.
3. Goldstein, J. L.; Brown, M. S.; Stradley, S. J.; Reiss, Y.; Gierasch, L. M., Nonfarnesylated tetrapeptide inhibitors of protein farnesyltransferase. *J Biol Chem* **1991,** 266, (24), 15575-8.
4. Qian, Y.; Sebti, S. M.; Hamilton, A. D., Farnesyltransferase as a target for anticancer drug design. *Biopolymers* **1997,** 43, (1), 25-41.
5. Stradley, S. J.; Rizo, J.; Gierasch, L. M., Conformation of a heptapeptide substrate bound to protein farnesyltransferase. *Biochemistry* **1993,** 32, (47), 12586-90.
6. Wilhelm, j. E.; Vale, R. D., RNA on the move: The mRNA localization pathway. *J. Cell Biology* **1993,** 123, (269-274).

7. Mowry, K. L.; Cote, C. A., RNA sorting in *Xenopus* oocytes and embryos. *FASEB Journal* **1999,** 13, 435-445.
8. Mohr, E.; Richter, D., Dendritic and axonal mRNA trafficking. *Regulatory Peptides* **1993,** 45, 21-24.
9. Barbarese, E.; Brumwell, C.; Kwon, S.; Cui, H.; Carson, J. H., RNA on the road to myelin. *J. Neurocytology* **1999,** 28, 263-270.
10. Steward, O.; Schuman, E. M., Protein Synthesis at Synaptic Sites on Dendrites. *Annu. Rev. Neurosci.* **2001,** 24, 299-325.
11. Bratu, D. P.; Cha, B.-j.; Mhlanga, M. M.; Kramer, F. R.; Tyagi, S., Visualizing the distribution and transport of mRNAs in living cells. *Proc. Natl. Acad. Sci.* **2003,** 100, (23), 13308-13313.
12. Santangelo, P. J.; Nix, B.; Tsourkas, A.; Bao, G., Dual FRET molecular beacons for mRNA detectionin living cells. *Nucleic Acids Res.* **2004,** 32, (6), e57.
13. Nitin, N.; Santangelo, P. J.; Kim, G.; Nie, S.; Bao, G., Peptide-linked molecular beacons for efficient delivery and rapid mRNA detection in living cells. *Nucleic Acids Res.* **2004,** 32, (6), e58.
14. Serganov, A.; Keiper, S.; Malinina, L.; Tereshko, V.; Skripkin, E.; Hobartner, C.; Polonskaia, A.; Phan, A. T.; Wombacher, R.; Micura, R.; Dauter, Z.; Jaschke, A.; Patel, D. J., Structural basis for Diels-Alder ribozyme-catalyzed carbon-carbon bond formation. *Nat Struct Mol Biol* **2005,** 12, (3), 218.
15. Unrau, P. J.; Bartel, D. P., RNA-catalysed nucleotide synthesis. *Nature* **1998,** 395, 260-263.
16. Marriott, J. H.; Mottahedeh, M.; Reese, C. B., Synthesis of 2'-thioadenosine. *Carbohydrate Research* **1991,** 216, (1), 257-269.
17. Zhu, X.-F.; Jr., H. J. W.; Scott, A. I., An Improved Transient Method for the Synthesis of N-Benzoylated Nucleosides. *Synthetic Communications* **2003,** 33, (7), 1233-1243.
18. Scaringe, S. A.; Wincott, F. E.; Caruthers, M. H., Novel RNA Synthesis Method Using 5'-*O*-Silyl-2'-*O*-orthoester Protecting Groups. *J. Am. Chem. Soc.* **1998,** 120, 11820-11821.
19. Nambiar, K. P.; Mitra, A., A MIld Method for Selective Cleavage of Tetrahydropyranyl Ethers in the Presence of Other Acid-Labile Functionalities. *Tetrahedron Letters* **1994,** 35, (19), 3033-3036.
20. Ogawa, Y.; Shibasaki, M., Selective Removal of Tetrahydropyranyl Ethers in the Presence of t-Butyldimethylsilyl Ethers. *Tetrahedron Letters* **1984,** 25, (6), 663-664.
21. Wagner, D.; Verheyden, J. P. H.; Moffatt, J. G., Preparation and Synthetic Utility of Some Organotin Derivatives of Nucleosides. *J. Org. Chem.* **1974,** 39, (1), 24-30.
22. Hotoda, H.; Takahashi, M.; Tanzawa, K.; Takahashi, S.; Kaneko, M., IP3 Receptor-Ligand 1: Synthesis of Adenophostin A. *Tetrahedron Letters* **1995,** 36, (28), 5037-5040.

Materials and Methods

General

All chemicals were purchased from Sigma-Aldrich, Alfa Aeser, TCI America, Dharmacon, or Lancaster Synthesis and used without further purification. Tetrahydrofuran was distilled over Na / benzophenone prior to use. Acetonitrile was distilled over CaH_2 for anhydrous work. Methanol, ethyl acetate, hexanes, absolute ethanol, pyridine, and toluene were used as received. Dichloromethane was used as received for general use and distilled over CaH_2 for anhydrous applications. Dry dioxane and DMF were used as received and stored under argon in the presence of 4 Å molecular sieves. Analytical thin layer chromatography (TLC) was conducted using 0.25 mm silica gel 60 F_{254} plates. Flash chromatography was conducted using silica gel (ICN SiliTech 32-63D).

Chapter 1:

p-Benzoyl-benzoic acid N-hydroxysuccinimidyl ester (BP-NHS)

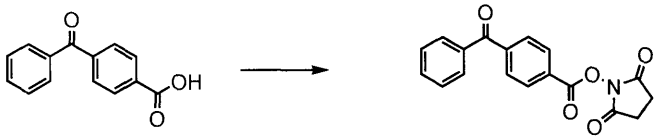

p-benzoylbenzoic acid was dissolved in 9:1 DCM / MeOH followed by 1.1 eq N-hydroxysuccinimide and 1.1 eq EDC-HCl. The solution was stirred at RT and monitored by TLC (2% MeOH in DCM). At completion, the reaction was diluted with DCM, washed with brine, and dried over Na_2SO_4. The solvent was removed *in vacuo* and the residue purified over silica using 0% to 5% MeOH in DCM to yield a white solid. R_f = 0.36 ^{1}H-NMR (400 MHz, $CDCl_3$) : δ 8.28 (2H, m), 7.90 (2H, m), 7.81 (2H, m), 7.63 (1H, m), 7.49 (2H, m), 2.94 (4H, s)

BP-Hydrazide

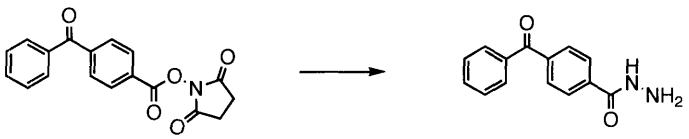

BP-NHS was dissolved in 10 mL DCM and slowly added to a solution of 20 eq. hydrazine in 5:1 DCM / EtOH over 7 minutes. The reaction was stirred at RT for two hours until ESI-MS showed complete consumption of the starting material and only product. The solution was concentrated *in vacuo* and redissolved into EtOAc. The organic later was washed twice with brine and dried over Na_2SO_4. Removal of the solvent yielded a white solid. ^{1}H-NMR (400 MHz, DMSO-D_6) δ 10.00 (1H, s), 7.97 (2H, d, J = 8 Hz), 7.80-7.68 (5H, m), 7.58 (2H, t, J = 8 Hz), 4.66 (2H, bs) ^{13}C-NMR (100 MHz, DMSO-D_6) δ 195.4, 164.9, 139.0, 136.7, 136.6, 133.0, 129.7, 129.5, 128.7, 127.2 ESI-MS $[M+H]^+$ calc 241.1 found 241.1

BP-4AB

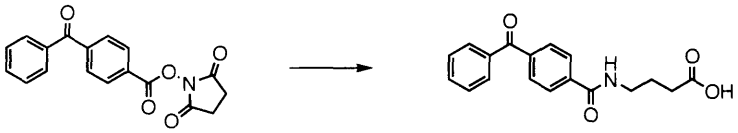

1.2 eq. 4-aminobutyric acid was dissolved in water and added to a solution of BP-NHS in 2 volumes THF. A cloudy solution resulted that slowly became clear as the reaction progressed. The reaction was monitored by TLC (5% MeOH in DCM with 1% AcOH) and the solvent removed *in vacuo* upon completion and the residue dissolved in DCM. The organic layer was washed twice with brine and dried over Na_2SO_4. The residue was purified over silica using 0% to 5% MeOH in DCM to obtain a white solid. R_f = 0.24
^{1}H-NMR (500 MHz, $CDCl_3$ / MeOD): δ 7.89-7.87 (2H, m), 7.80-7.74 (4H, m), 7.60-7.57 (1H, m), 7.58-7.45 (2H, m), 3.47 (2H, t, J= 7 Hz), 2.41 (2H, t, J= 7 Hz), 1.93 (2H, pent, J= 7 Hz) ^{13}C-NMR (125 MHz, $CDCl_3$ / MeOD): δ 196.7, 176.5, 167.4, 140.0, 137.8,

137.0, 133.1, 130.2, 130.1, 129.9, 129.8, 128.6, 127.2, 39.8, 31.8, 24.3 ESI-MS $[M-H]^-$ calc. 310.11 found 310.11

BP-4AB-NHS

BP-4AB was dissolved in 5:1 DCM / MeOH followed by 1.4 eq NHS and 1.4 eq EDC-HCl. The solution was stirred at RT and monitored by TLC (4% MeOH / DCM) with the product appearing at R_f = 0.35. Upon completion, the reaction was diluted with DCM, washed with brine, and dried over Na_2SO_4. The residue was purified over silica using 0% to 5% MeOH in DCM. Material used for protein labeling was purified a second time by reverse phase semi-preparative HPLC. Using a 300 Å column with a gradient of 25% to 85% acetonitrile in water with 0.1% TFA at 4.7 mL / min, the product eluted at 11 minutes as monitored by UV absorbance at 254 nm. The product was lyophilized to yield a white powder. ^{1}H-NMR (400 MHz, $CDCl_3$) δ 7.90-7.78 (6H, m), 7.62 (1H, t, J = 8 Hz), 7.50 (2H, t, J=8 Hz), 6.86 (1H, t, J=6 Hz), 3.60 (2H, q, J=6 Hz), 2.85 (4H, s), 2.75 (2H, t, J= 7 Hz), 2.17-2.12 (2H, m) ^{13}C-NMR (100 MHz, $CDCl_3$): δ 196.3, 169.5, 168.7, 167.2, 140.2, 137.8, 137.2, 133.1, 130.3, 128.7, 127.2, 39.1, 28.7, 25.8, 24.5 ESI+MS $[M+H]^+$ calc. 409.14 found 409.14

BP-4AB-Hydrazide

BP-4AB was dissolved in 4:1 DCM / MeOH followed by the addition of 10 eq. hydrazine. 1.4 eq. EDC-HCl was then added and the solution stirred at RT for 1 hour. TLC (4% MeOH in DCM) showed complete conversion to product at R_f = 0.21. The reaction was diluted with DCM, washed with brine, and dried over Na_2SO_4. Purification

was done first by silica column using a gradient of 0% to 5% MeOH in DCM and later by semi-preparative HPLC using the same conditions as for BP-4AB-NHS with an elution time of 7 minutes. ^{1}H-NMR (300 MHz, $CDCl_3$ / MeOD) δ 9.6 (1H, s), 8.5 (1H, s), 7.92 (2H, t, J = 8 Hz), 7.77 (4H, m), 7.56 (1H, t, J = 7 Hz), 7,47 (2H, t, J = 7 Hz), 2.85 (2H, m), 1.83 (2H, m) ESI-MS $[M+H]^+$ calc. 326.2 found 326.2

p50AP in pRSETB

The acceptor peptide (AP) was appended to the C-terminus of truncated murine p50 by PCR with the forward primer 5-GATAAGGATCCGGCCCCATACCTTGAAATATT, which introduced a 5' BamHI site, and the reverse primer 5′-TCATGAATTCTTACTCGTGCCACTCGATCTTCTGGGCCTCGAAGATGTCGTTCAGGCCG CCGCCGGAGGACTCCTTGTACAGCTCCTTCTGGCGTTTCCTTTG, containing the AP sequence, stop codon, and 3' EcoRI site for cloning. Taq polymerase was used the amplify the p50 gene using a PCR cycle consisting of a 2 min 95 °C initial denaturation, 24 cycles of 30 sec 95 °C, 30 sec 50-62 °C annealing using 0.5 °C increments / cycle, 1.5 min 72 °C elongation, and a 3 min 72 °C final elongation step. A 1% agarose gel was used to purify the resulting transcript. A band at ~1 kb was excised and the DNA extracted using a Qiagen gel extraction kit according to manufacturers instructions. pRSETB was prepared for cloning by double digest using EcoRI and BamHI at 37 °C for 2.5 hours in NEB EcoRI buffer in the presence of BSA. The plasmid was purified on a 0.8 % agarose gel and purified by gel extraction. The plasmid was treated with alkaline phosphotase in NEB Buffer 3 for 1 hour at 37 °C. DNA was purified using a Qiagen PCR cleanup kit and the product eluted with 30 μL EB buffer. The insert was ligated to the plasmid using T4 DNA ligase at RT for 3 hours in T4 ligase buffer. The resulting plasmids were transformed into DH5α cells by 45 sec 42 °C heat shock followed by immediate rescue in 500 μL SOB at 37 °C with shaking for 40 min. Bacteria were plated on LB-Amp plates and grown overnight at 37 °C. Colonies were selected and grown in 5 mL LB-Amp cultures at 37 °C overnight. Plamsids were isolated by Qiagen miniprep kit according to manufacturer's instructions. Plasmids were confirmed by BamHI / EcoRI digest and DNA sequencing.

p50Ala in pRSETB

The AP lysine was mutated to alanine using site directed mutagenesis. Pfu Turbo polymerase (Invitrogen) was used with the primers 5′-CGACATCTTCGAGGCCCAGGCGATCGAGTGGCACG and 5′-CGTGCCACTCGATCGCCTGGGCCTCGAAGATGTCG with the PCR cycle 30 sec 95 °C initial denaturation, 18 cycles 30 sec 95 °C denaturation, 1 min 55 °C annealing, 15 min 68 °C elongation, followed by a 8 min 68 °C final elongation step. The resulting plasmid was digested for 2 hours at 37 °C with DpnI to degrade the wild type plasmid. Plasmids were transformed into XL1 Blue by heat shock, rescued in SOB at 37 °C for 30 min, and plated on LB-Amp plates at 37 °C overnight. Single colonies were miniprepped from 5 mL LB-Amp cultures according to manufacturer's instructions, and confirmed by analytical digestion and sequencing.

Transfer of p50AP and p50Ala from pRSETB to pET21b(+)

Both p50AP and p50Ala in pRSETB were excised by EcoRI / BamHI double digest followed by 0.5% agarose gel purification and gel extraction. pET21b(+) was digested with BamHI and EcoRI and also subjected to agarose gel purification followed by alkaline phosphotase treatment as described earlier. The inserts were ligated using a 2 hour T4 ligase reaction at ambient temperature. Plasmids were transformed into DH5α by heat shock, rescued in SOB at 37 °C for 40 min, and plated on LB-Amp plates overnight a 37 °C. Colonies were selected and mini-prepped from 5 mL LB-Amp cultures grown overnight at 37 °C. Plasmids were confirmed by analytical digest and sequencing. As pET21b(+) encodes a C-terminal His_6-tag for purification, the stop codon following the AP tag was removed by site-directed mutagenesis using the primers 5'-GATCGAGTGGCACGAGAAGAATTCGAGCTCCG AND 5′-CGGAGCTCGAATTCTTCTCGTGCCACTCGATC to leave a small linker between the AP and the His-tag. The previous mutagenesis PCR sequence was modified to increment the

annealing temperature by 0.5 °C after each round and DH5α was used for transformations and plasmid isolation. Sequences were confirmed for each plasmid.

Expression of BirA

BirA in pBTac2 was transformed into *E. coli* strain JM109 by 45 second, 42 °C heat shock followed by immediate rescue in 0.5 mL SOB at 37 °C with shaking for 40 minutes. 0.1 mL was then plated on LB-Ampicillin plates and incubated at 37 °C overnight. Single colonies were chosen and grown in Luria Bertani broth supplemented with 100 μg/mL ampicillin (LB-Amp) at 37 °C to saturation. This culture was then diluted 1:1000 into LB broth supplemented with ampicillin (100 μg/mL). BirA was grown to an OD_{600} = 0.9 at 37 °C with shaking (220 rpm) and induced with IPTG to a final concentration of 0.4 mM. Induced BirA cultures were grown an additional 4 hours at 30 °C with shaking. Cells were collected by centrifugation followed by lysis by sonication at 4 °C (four 30-second pulses at half-maximal power with 1 minute between each pulse) in lysis buffer (50 mM Tris pH 7.8, 300 mM NaCl) containing 5 mM phenylmethyl-sulfonyl fluoride (PMSF) and protease inhibitor cocktail (Calbiochem). The His_6-tagged enzyme was purified from the lysate using Ni-NTA agarose (Qiagen). Fractions containing enzyme were combined and dialyzed against PBS pH 7.4. To remove biotin-AMP ester in the active site, the protein was incubated at 30 °C in the presence of 1 mM synthetic AP and 4 mM ATP for 1 hour. The protein was then repurified by Ni-NTA column and dialyzed against PBS pH 7.4.

Expression of CFP and p50 proteins

CFPAP, CFPAla, p50AP, and p50Ala (all in pRSETB) were expressed in *E. coli* strain BL21(DE3). Bacteria were transformed by 45 second heat shock at 42 °C followed by rescue in 0.5 mL SOB for 30 minutes and plated on LB-Amp plates overnight at 37 °C. Bacteria were grown at 37 °C to an OD_{600} = 0.2 and induced with IPTG to a final concentration of 0.4 mM followed by incubation overnight at 25 °C with shaking. Cells were collected by centrifugation followed by lysis by sonication at 4 °C (four 30-second

pulses at half-maximal power with 1 minute between each pulse) in lysis buffer (50 mM Tris pH 7.8, 300 mM NaCl) containing 5 mM phenylmethyl-sulfonyl fluoride (PMSF) and protease inhibitor cocktail (Calbiochem). The His_6-tagged enzyme was purified from the lysate using Ni-NTA agarose (Qiagen). Fractions containing enzyme were combined and dialyzed against PBS pH 7.4. AP-tagged proteins were then filtered over a column of streptavidin agarose four times to remove pre-biotinylated proteins.

Biotinylation assays

1 μM AP-tagged protein was treated with 1 μM BirA in the presence of 4 mM ATP and 1 mM biotin in 50 mM bicine buffer pH 8.2 supplemented with 5 mM $Mg(OAc)_2$ for 1 hour at 30 °C. The reaction was then diluted with protein loading buffer and heated to 100 °C for 15 minutes. Samples were subjected to 12% SDS-PAGE gel followed by western blot. The blot was blocked with 3% BSA in TBS-T for 1 hour at ambient temperature. 2 μg / mL Streptavidin-HRP conjugate in 3%BSA / TBS-T was applied to the blot for 15 minutes at ambient temperature followed by three 5-minute washes in TBS-T to remove unbound streptavidin. The blot was then visualized using Supersignal West Luminol (Pierce).

Ketone biotinylation and hydrazide conjugation

AP-tagged proteins in 50 mM bicine pH 8.2 with 5 mM $Mg(OAc)_2$ were treated with 1 μM BirA, 4 mM ATP, and 200 μM racemic ketone biotin for 3 hours at 30 °C. The pH was then adjucted to 6.2 with 0.1 M HCl prior to adding 1 mM hydrazide probe. The reaction was incubated at 30 °C for 12-15 hours before the hydrazide adduct was reduced by 15 mM $NaBH_3CN$ at 4 °C for 1.5 hours. Samples were diluted with protein loading buffer and heated to 100 °C for 15 minutes prior to loading onto 12 % SDS-PAGE. Fluorescein hydrazide was visualized in-gel by fluorescence scanning on a STORM fluorescence scanner. BPBio-hydrazide-treated samples were transferred by western blot and visualized using the same protocol as for the biotinylation assay.

Crosslinking Assays

AP-tagged proteins were subjected to the ketone biotinylation and hydrazide conjugation protocol described above. Following hydrazide conjugation, samples were placed on ice for 2-30 minute UV irradiation. Following irradiation, the hydrazide conjugate was reduced and 8% SDS-PAGE performed. BP-hydrazide and BP-linker hydrazide were visualized by either silver or coomassie staining. BPBio hydrazide samples were detected by either silver staining or by western blot and streptavidin-HRP detection as described above.

Chapter 2:

5(6)-carboxyfluorescein

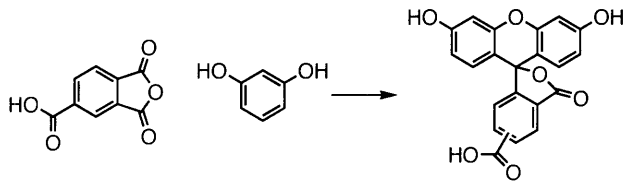

Trimellitic anhydride (26.5 mmol, 5.09 g) and resorcinol (53 mmol, 5.84 g) Were stirred overnight at 80°C in 80 mL methanesulfonic acid. The resulting red solution was allowed to cool to room temperature before pouring into 300 mL of ice water with stirring. A orange-yellow solid precipitated. The solid was collected by filtration and rinsed three times with water, Drying of the solid at 110° C or high vacuum resulted in a yellow-orange solid in near quantitative yield as a near 50-50 mixture of 5- and 6-carboxyfluorescein. ^{1}H-NMR (300 MHz, DMSO): δ 8.40 (1H, m), 8.30 (1H, dd, J_1=8.1 Hz, J_2=1.5 Hz), 8.22 (1H, dd, J_1=8.1 Hz, J_2=1.5 Hz), 8.10 (1H, dd, J_1=8.1 Hz, J_2=0.6 Hz), 7.66 (1H, m), 7.39 (1H, dd, J_1=8.1 Hz, J_2=0.6 Hz), 6.72-6.52 (12H, m)

Bis-pivanoyl-6-carboxyfluorescein diisopropylammonium salt

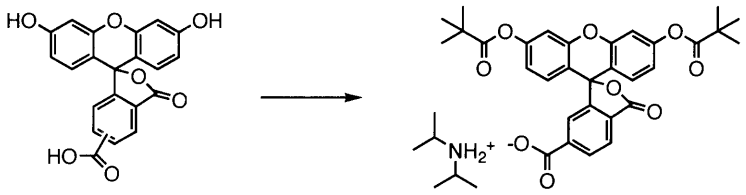

5(6)-carboxyfluorescein (39.85 mmol, 15 g) was stirred at reflux in a mixture of trimethylacetic anhydride (159.4 mmol, 30g) and triethylamine (120 mmol, 12 g) and monitored by TLC (1% AcOH, 5% MeOH in DCM) until a single spot was present. The solution was cooled room temp followed by the addition of 15 mL water and 15 mL THF. The solution was stirred vigorously for 2 hours and diluted in 150 mL ether. The organic layer was washed three times with 1.4 M, pH 7 phosphate buffer, once with 1M

HCl, and twice with brine. The organic layer was dried over $MgSO_4$ and the solvent removed *in vacuo*. The resulting syrup was dissolved into 40 mL EtOH and 20 mL diisopropylamine and cooled to -20° C. A white solid formed which was collected by vacuum filtration, washed twice with cold EtOH and once with cold acetone. The sticky white residue was then dried to a white powder *in vacuo*. . ^{1}H-NMR (300 MHz, $CDCl_3$): δ 8.25 (1H, dd, J_1=8.1 Hz, J_2=1.5 Hz), 7.98 (1H, dd, J_1=7.8 Hz, J_2=0.6 Hz), 7.68 (1H, m), 7.02 (2H, d, J=2.1 Hz), 6.83 (2H, d, 8.4 Hz), 6.74 (2H, dd, J_1=8.7 Hz J_2=2.1 Hz), 3.21 (2H, sept, J=6.3 Hz), 1.35 (18H, s), 1.22 (12H, d, J=6.6 Hz)

6-Carboxyfluorescein

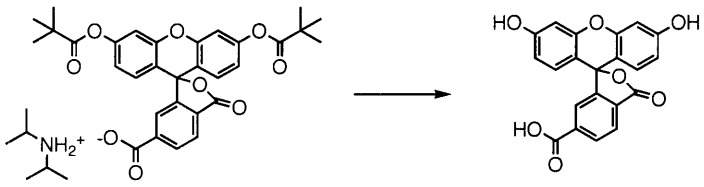

Diisopropylammonium Bis-pivanoyl-6-carboxyfluorescein was dissolved in a minimal volume of methanol followed by the addition of 2M aq. NaOH. A deep red-black color developed. The solution was stirred until TLC (1% AcOH, 5% MeOH in DCM) showed complete removal of the pivolate groups. Methanol was removed *in vacuo* and the resulting aqueous solution treated with 1M HCl with stirring to precipitate the 6-cabroxyfluorescein as a voluminous yellow solid. The solid was collected by filtration and dried under high vacuum to a yellow solid. ^{1}H-NMR (300 MHz, DMSO): δ 10.18 (bs, COOH), 8.22 (1H, d, J=8 Hz), 8.11 (1H, d, J=8 Hz), 7.65 (1H, s), 6.70-6.53 (6H, m), 3.40 (bs, OH)

5-carboxyfluorescein

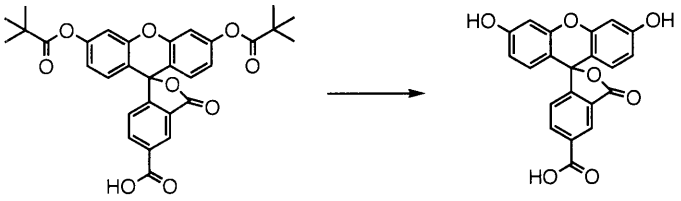

The pivolate syrup was completely depleted of 6-carboxyfluorescein by repeated precipitation with diisopropylamine in ethanol at -20 °C. The remaining syrup was dissolved in THF to which 2M aq. NaOH was added. The solution was allowed to stir at RT as a deep red-black color developed. The solution was stirred until TLC (1% AcOH, 5% MeOH in DCM) showed complete removal of the pivolate groups. THF was removed *in vacuo* and the resulting aqueous solution treated with 1M HCl with stirring to precipitate the 5-cabroxyfluorescein as a voluminous yellow solid. The solid was collected by filtration and dried under high vacuum to a yellow solid. ^{1}H-NMR (400 MHz, DMSO): δ 10.25 (bs, COOH) 8.40 (1H, d, J=1.6 Hz), 8.29 (1H, dd, J_1= 8 Hz , J_2= 1.6 Hz), 7.40 (1H, d, J=8 Hz), 6.72 (1H, d, J=2 Hz), 6.61 (1H, d, J= 9Hz), 6.55 (1H, dd, J_1= 9 Hz, J_2= 2 Hz), 4.21 (bs, OH)

5-carboxyfluorescein dimethyl ester

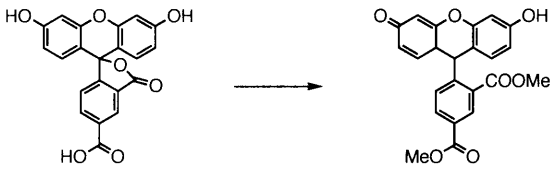

5-CF impurities in some 6-CF batches were observed by 1H-NMR to be converting to the desired dimethyl esters and methyl ethers. As such, an attempt was made to make use of the stock of 5-CF we have available. 5-CF was refluxed overnight in MeOH with catalytic sulfuric acid. The resulting solution was concentrated and diluted in DCM, washed with 100 mM pH 7 phosphate buffer and brine, then dried over $MgSO_4$. Removal

of the solvent yielded a red solid. ^{1}H-NMR ($CDCl_3$): δ 8.91 (d, 1H), 8.43 (dd, 1H), 7.48 (d, 1H), 7.23-7.13 (m, 6H), 4.06 (s, 3H), 3.67 (s, 3H)

5-carboxyfluorescein methyl ether

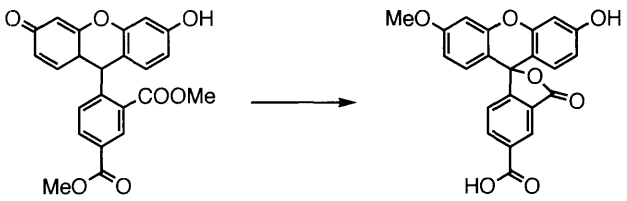

5-CF Dimethyl ester was dissolved into dry DMF in the presence of Cs_2CO_3. MeI was added and the reaction stirred until completion. The solution was diluted in ethyl acetate and washed with citric acid and brine. The organic layer was dried over $MgSO_4$ and the solvent removed in vacuo. 1M NaOH was added along with a minimal amount of methanol and allowed to stir overnight. The product was re-precipitated using 1M HCl and collected by filtration. ^{1}H-NMR(MeOD): δ 8.59 (d, 1H), 8.4 (d, 1H), 7.30 (d, 1H), 6.86 (t, 1H), 6.7-6.6 (m, 5H), 3.85 (s, 3H)

6-carboxyfluorescein dimethyl ester

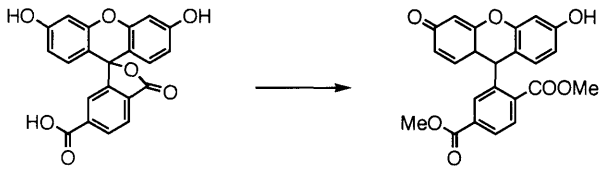

Purified 6-carboxylfuorescein was refluxed overnight in methanol in the presence of catalytic sulfuric acid. Following washings and extraction into dichloromethane, the desired compound was attained in 60-75% yield. ^{1}H-NMR (300 Mhz, $CDCl_3$): 8.32 (s, 2H), 7.98 (s, 1H), 6.93-6.77 (m, 6H), 3.94 (s, 3H), 3.65 (s, 3H), 3.24 (bs)

6-carboxyfluorescein methyl ether

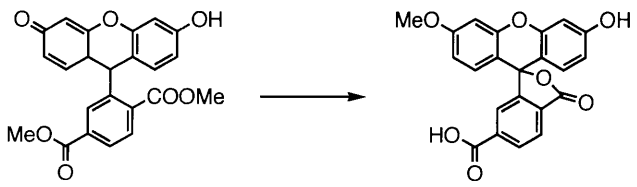

6-carboxyfluorescein dimethyl ester was treated with iodomethane in the presence of cesium carbonate followed by ester cleavage in 2M NaOH. Precipitation with 1M HCl yielded the desired compound in about 50% yield. ^{1}H-NMR (300 Mhz, MeOD): 8.30 (d, 1H, J=7.8 Hz), 8.07 (d, 1H, J=7.8), 7.72 (s, 1H), 6.87 (s, 1H), 6.71-6.43 (m, 5H), 3.84 (s, 3H) ESI-MS: $[M+H]^+$ calc. 391.0812 found 391.0813

6-carboxyfluorescein methyl ether dibenzyl phosphate

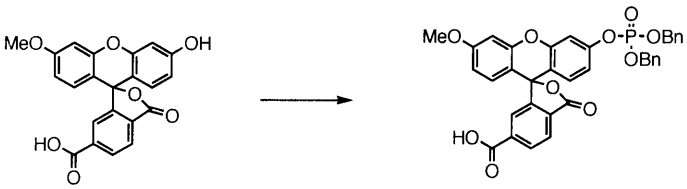

6-carboxyfluorescein was dissolved in dry acetonitrile under argon with 3 eq. of dicyanoimidazole. 2 eq. of dibenzyl-diisopropyl-phosphoramidite was added by syringe and the solution stirred at RT for 45 min. The resulting phosphite was oxidized by the portion-wise addition of 4 eq. mCPBA and stirred at RT for an additional 30 min. The solution was diluted with DCM, washed sequentially with 1.5 M Na_2SO_3, 1M HCl, and brine followed by drying over Na_2SO_4. The solution was concentrated *in vacuo* and purified over silica using a gradient of 0% to 5% MeOH in DCM with 1% AcOH. . ^{1}H-NMR (400 MHz, $CDCl_3$): δ 8.35 (1H, d), 8.13 (1H, d), 7.85 (1H, s), 7.34 (10H, m), 7.08 (1H, s), 6.68 (2H, m), 6.67 (3H, m), 5.16 (4H, dd), 3.86 (1H, s)

6-carboxyfluorescein methyl ether dibenzyl phosphate N-hydroxysuccimidyl ester

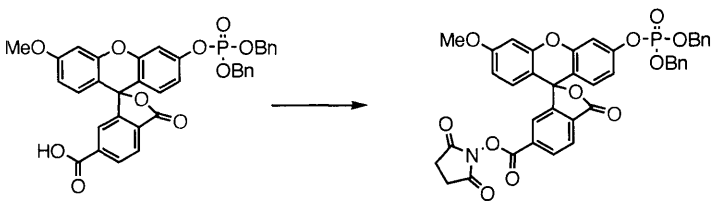

6-carboxyfluorescein methyl ether dibenzyl phosphate was dissolved in DCM with 2 eq. N-hydroxysuccinimide and 1.2 eq. EDC-HCl and stirred at RT. The reaction was monitored by TLC (EtOAc) with additional NHS and EDC-HCl added until completion 0.5 eq at a time. The solution was diluted with DCM, washed with brine, and dried over Na_2SO_4. The product was purified over silica (50% to 100% EtOAc in hexanes) and dried under high vacuum. R_f = 0.76 in EtOAc. 1H-NMR (300 MHz, $CDCl_3$): δ 8.39 (1H, dd, J_1= 8Hz J_2= 1 Hz), 8.16 (1H, d, J= 8 Hz), 7.88 (1H, s), 7.32 (10H, m), 7.10 (1H, s), 6.78 (2H, m), 6.66 (3H, m), 5.13 (4H, dd, J_1= 9 Hz, J_2= 1 Hz), 3.86 (3H, s), 2.89 (4H, s)

6CFME-PhosOH2

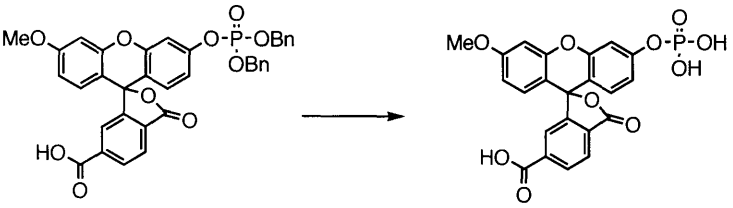

6NHS-CFME-Phos-OBn2 was added to an oven-dried round bottom flask with stirbar. The flask was evacuated and refilled with argon four times followed by the addition of DCM distilled fresh over CaH_2. 10 eq. of TMS-Br was then added by syringe and stirred at RT. A deep brown color developed almost immediately. At 2 hours, the reaction was diluted with DCM and extracted with water. The aqueous layer was washed with DCM prior to solvent removal *in vacuo* to provide the product as a faint yellow solid. The solid was tested against alkaline phosphotase and recognized by the enzyme.

6NHS-CFME-PhosOH2

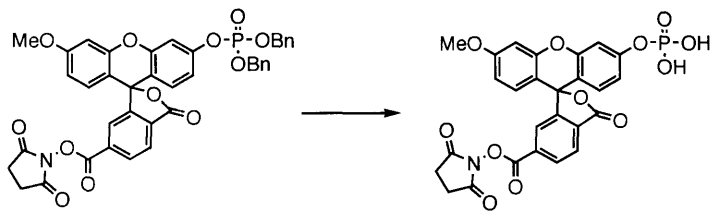

6NHS-CFME-Phos-OBn2 was added to an oven-dried round bottom flask with stirbar. The flask was evacuated and refilled with argon four times followed by the addition of DCM distilled fresh over CaH_2. 10 eq. of TMS-Br was then added by syringe and stirred at RT. A deep brown color developed almost immediately. At 2 hours, the reaction was diluted with DCM and extracted with water. The aqueous layer was washed with DCM prior to solvent removal *in vacuo* to provide the product as a faint yellow solid. The solid was tested against alkaline phosphotase and recognized by the enzyme.

5C-TPF-OEt2

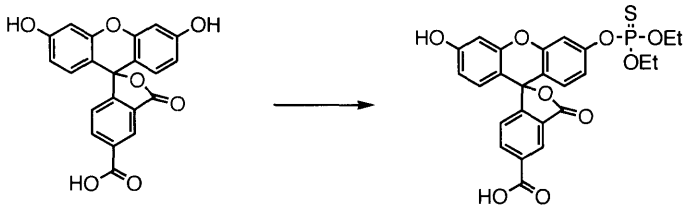

5-carboxyfluorescein was dissolved in dry DMF and cooled in an ice bath. 4 eq. of NaH was added in portions and the reaction stirred on ice until gas evolution ceased. 2.2 eq of chloro-diethyl-thiophosphate was then added and the solution brought to RT. The reactionw as diluted with DCM, washed with water and brine, and dried over Na_2SO_4. The product was purified over silica using 0% to 5% MeOH in DCM with 1% AcOH. TLC with 5% MeOH and 1% AcOH in DCM produced a single spot at R_f= 0.8. ^{1}H-NMR (400 Mhz, $CDCl_3$) δ 8.71 (1H, s), 8.36 (1H, d, J = 8 Hz), 7.27-6.56 (7H, m), 4.28-4.20 (4H, m), 1.42-1.35 (6H, m) ^{31}P-NMR (161 Mhz, $CDCl_3$) δ 62.8 ESI-MS: 529.1 $[M+H]^+$

5NHS-TPF-OEt2

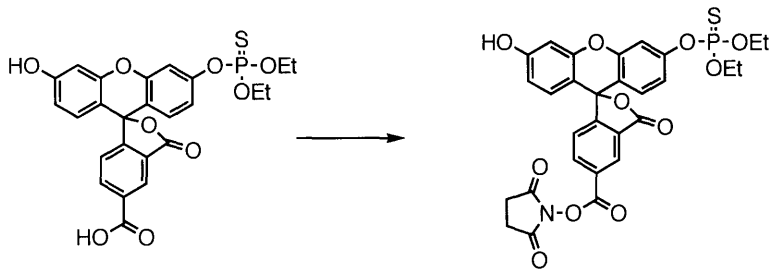

5C-TPF-OEt2 was dissolved in acetonitrile followed by the addition of 2 eq. NHS and 2 eq. EDC-HCl. The solution was stirred for 3 hours before being diluted with DCM, washed with water and brine, and dried over Na_2SO_4. Purification was done by silica column using a gradient of 0% to 5% MeOH in DCM with 1% AcOH to provide a yellow solid. . ^{1}H-NMR (400 Mhz, $CDCl_3$) δ 8.73 (1H, s), 8.34 (1H, d, J = 8 Hz), 7.32-6.52 (7H, m), 4.25-4.20 (4H, m), 2.93 (4H, s), 1.37-1.34 (6H, m) ^{31}P-NMR (161 Mhz, $CDCl_3$) δ 62.7 ESI-MS: 626.2 $[M+H]^+$

6C-TPF-OBn2

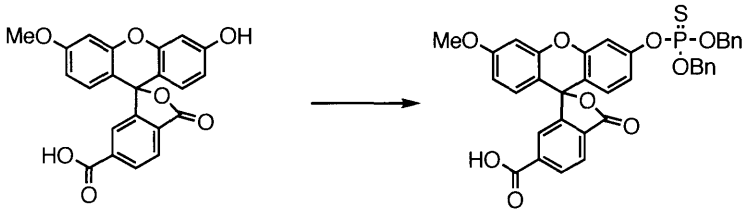

6CFME and 3 eq. DCI were combined in an oven-dried flask with stirbar. The flask was evacuated and refilled with dry argon 3 times. Freshly distilled, dry acetonitrile was added by syringe followed by 2 eq. dibenzyl-diisopropyl-phosphoramidite. The solution was stirred for 30 minutes at which point ESI-MS (pos. mode) showed a single peak corresponding to a phosphite product at m/z 635 $[M+H]^+$. The flask was opened briefly to add 6 eq. elemental sulfur and stirred at RT overnight. The phosphite gradually vanished as the thiphosphate peak appeared at m/z 677 $[M+H]^+$. The reaction was diluted with DCM, washed with water and brine, and dried over $MgSO_4$. The solvent was removed *in*

vacuo, the residue suspended in acetonitrile, and the solids removed by centrifugation. The supernatant was purified by reverse phase semi-preparative HPLC using a gradient of 25% to 85% acetonitrile in water with 0.1% TFA over 20 minutes with a flow of 4.7 mL / min. The product eluted at 19 min as monitored by absorbance at 254 nm. The product was lyophilized to an reddish-orange oil. ^{1}H-NMR (300 Mhz, $CDCl_3$) δ 8.34 (1H, dd, J_1= 8 Hz, J_2= 1 Hz), 8.12 (1H, d, J = 8 Hz), 7.87 (1H, s), 7.35-7.30 (10H, m), 7.06 (1H, s), 6.80-6.65 (5H, m), 5.20-5.16 (4H, m), 3.85 (3H, s) ^{31}P-NMR (121 Mhz, $CDCl_3$) δ 63.7

6NHS-TPF-OBn2

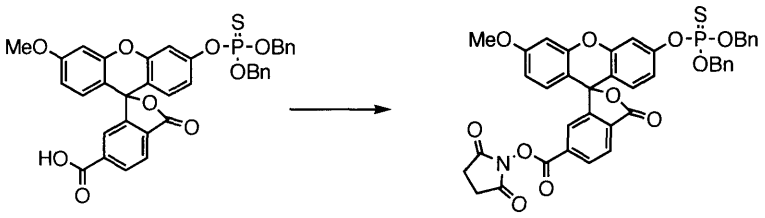

6C-TPF-OBn2 was dissolved in DCM with 1.4 eq. NHS at RT. 1.4 eq. EDC-HCl was then added and the reaction stirred for 3 hours. ESI-MS showed complete conversion to product. The reaction was diluted with DCM, washed three times with brine, and dried over Na_2SO_4. The solvent was removed *in vacuo* and the residue dissolved in acetonitrile for HPLC purification as described for 6C-TPF-OBn2 with an elution time of 21 min. ^{1}H-NMR (400 Mhz, $CDCl_3$) δ 8.40 (1H, dd, J_1= 8 Hz, J_2= 1 Hz), 8.17 (1H, d, J = 8 Hz), 7.92 (1H, s), 7.35-7.30 (10H, m), 7.08 (1H, s), 6.80-6.65 (5H, m), 5.20-5.16 (4H, m), 3.86 (3H, s), 2.88 (4H, s)

6NHS-TPF

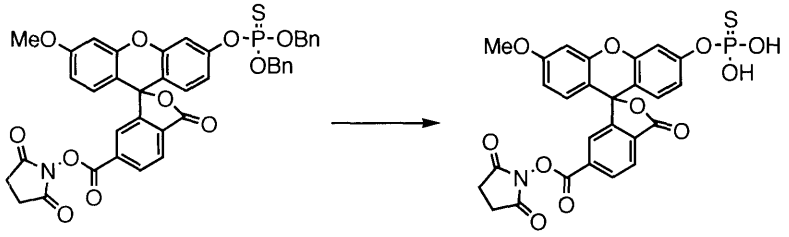

6NHS-TPF-OBn2 was dissolved in dry acetonitrile under argon. 20 eq. TMS-Br was added by syringe and the solution heated to 55 °C for 2 hours. The reaction was quenched with MeOH and the crude purified by semi-prep HPLC under the same conditions as 6C-TPF-OBn2 with elution times of 9 min. corresponding to the fully deprotected product and 12 min. for the mono-benzylated product. Both compounds were flash frozen and lyophilized to yellow solids.

Alkaline phosphatase assay

100 μM FDP or 16 μM 6CFME-phosphate were monitored at 30 °C in 50 mM Tris-HCl pH 8.0 supplemented with 25 mM $MgCl_2$ on a SAFIRE plate reader in the presence or absence of 0.1 unit CIP. Excitation at 490 nM with monitoring from 495-550 nM in 5 nM increments and a 5 nM emission bandwidth. Fluorescence measurements were taken from the bottom of a 96 well plate at 60 second intervals for 60 minutes.

RNA translation and purification

1 μg of the library template (2 x 10^{13} molecules) was used in a 20 μL RNA trancription reaction using an Ampliscribe T7-Flash kit according to manufacturer's instructions. The reaction was conducted at 42 °C for 1 hour prior to purification on a 7% PAGE-Urea gel. RNA was located within the gel by UV shadowing against a silica plate and excised. The RNA-containing gel fragment was crushed and allowed to equilibriate with DEPC-treated water for 6 hours at 4 °C. The RNA was ethanol precipitated and resuspended in RNA binding buffer (50 mM Tris-HCl pH 8, 50 mM NaCl, 50 mM KCl).

Library activity assays

Fluorescein diphosphate (FDP), 6,8-difluoro-4-methylumelliferyl phosphate (DiFMUP), and *9H*-(1,3-dichloro-9,9-dimethylacridin-2-one-7-yl) phosphate (DDAO) were obtained from Molecular Probes, and stock solutions were prepared according to their instructions. 6CFME-phosphate was prepared as a 10 mM stock solution in 50 mM Tris-HCl pH 7.4. RNA activity assays were conducted with the commercial probes in 50 mM Tris-HCl pH 7.4 in the presence or absence of 25 mM $MgCl_2$ at 30 °C. 6CFME-phosphate assays were conducted under the same conditions except that the pH was set to 8.0. FDP and 6CFME-Phosphate were exited at 490 nM and fluorescence monitored from 495-530 nM in 5 nM increments with a 2.5 nM emission bandwidth. DDAO was excited at 646 nM and monitored from 650-670 nM in 5 nM increments with a 2,5 nM emission bandwidth. DiFMUP was excited at 358 nM and monitored from 435-475 nM in 5 nM increments with a 2.5 nM emission bandwidth. All probes were used at a final concentration of 100 μM. Positive controls to show full fluorescence turn on were treated with 0.1 unit of calf intestinal phosphatase (New England Biolabs). 1 μg RNA was used per 25 μL reaction. Reactions were run in clear, flat bottomed 96 well plates and sealed with clear tape. Fluorescence measurements were taken from the bottom of the well at 1-2 minute intervals with orbital shaking (10 seconds shaking, 5 seconds settle time) between each measurement using a SAFIRE plate reader.

Aptamer Selection Protocol

Both negative and positive selection beads were pre-blocked with 3% BSA in RNA binding buffer (50 mM Tris-HCl pH 8.0, 50 mM NaCl, 50 mM KCl) for 20 minutes at 37 °C. The beads were spun down and washed twice with binding buffer. To 0.5 mg of pre-blocked negative selection beads, 0.2 nmol of the RNA library was applied in binding buffer. The RNA was incubated for 15 minutes at 37 °C and the beads removed by centrifugation. The supernatant was then applied to 0.5 mg of pre-blocked positive selection beads in for 30 min at 37 °C. The beads were spun down and washed 4 times with binding buffer containing 3% BSA and 0.1% Tween followed by 2 more washes with binding buffer alone. Bound RNA was eluted using 100 μM 6-carboxyfluorescein methyl ether phosphate in binding buffer at 37 °C for 15 min. The beads were removed

by centrifugation and RNA ethanol precipitated to remove fluorescein. The RNA was then converted back to DNA with the addition of a T7 promotor by RT-PCR using the primers 5'- GGATTTCGAAAGCCAGCTTAATGAGCAACG and 5'- AGCGGGTACCGCGTAATACGACTCACTATAGGAGTGGTTGCATGTACGCC. The RT-PCR cycle consisted of 1 30 minute RT reaction at 50 °C, 2 min at 94 °C, followed by 40 cycles of 15 sec 94 °C, 15 sec 64 °C, and 30 sec 66.5 °C. The product was either ethanol precipitated or purified using a Qiagen PCR cleanup kit.

Library Cloning

Both the library and pUC19 were sequentially digested overnight by KpnI followed by Csp45I. The resulting fragments were purified by agarose gel and extracted from the gel using a Qiagen gel extraction kit. Vector and insert were ligated using T4 DNA ligase and transformed into *E. coli* strain DH5α. Single colonies were chosen and grown in LB broth supplemented with ampicillin to saturation, and the plasmids isolated using a Qiagen miniprep kit. Plasmids were analyzed by analytical digest and sequencing.

Chapter 3:

3'O, 5'O-TIPDS-Adenosine

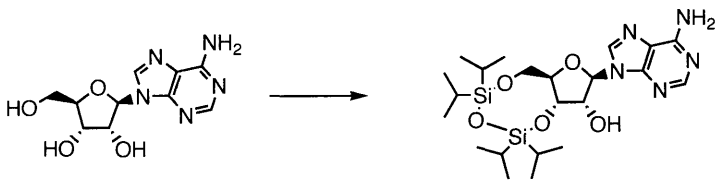

1.1 eq of 1,3-dichloro-1,1,3,3-tetraisopropyl-disiloxane was added to a suspension of adenosine in dry pyridine under argon and stirred at RT overnight. The solvent was removed *in vacuo* and the residue dissolved in DCM. The organic layer was washed with sat. $NaHCO_3$ and the aqueous layer extracted twice with DCM. The combined organic phases were dried over Na_2SO_4 and concentrated *in vacuo*. The resulting syrup was purified over silica (0% to 5% MeOH in DCM) and dried under vacuum to yield a dense, white solid. . ^{1}H-NMR (300 MHz, $CDCl_3$): δ 8.28 (1H, s), 7.97 (1H, s), 5.98 (3H, bs), 5.09-5.04 (1H, m), 4.58 (1H, d, J= 6 Hz), 4.17-4.00 (3H, m), 3.76 (1H, bs), 1.12-0.98 (28H, m)

N, N, 2'O-tribenzoyl, 3'O-5'O-TIPDS Adenosine

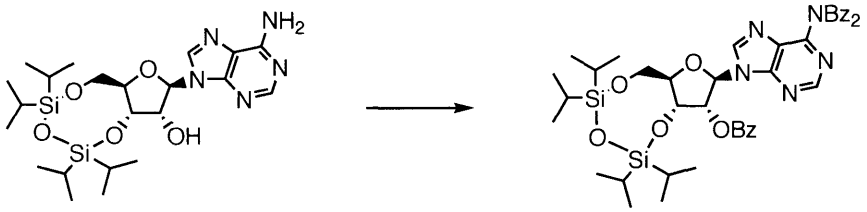

To a solution of TIPDS-Adenosine in pyridine was added 5 eq of Bz-Cl. The solution was allowed to stir at RT for 16 hours prior to the addition of water. The mixture was stirred for an additional 30 minutes and then had the solvent removed in vacuo. The resulting material was dissolved in DCM and washed with saturated sodium bicarbonate and dried over magnesium sulfate. Purification over silica column using 1:1, 2:1, 1:0 ethyl acetate/hexanes produced the desired product as a white foam. Yields are nearly

quantitative. 1H-NMR (CDCl3) δ 8.60 (s, 1H), 8.23 (s, 1H), 8.1 (m, 2H), 7.87 (m, 4H), 7.6 (m, 1H), 7.46 (m, 4H), 7.37 (m, 4H), 6.2 (s, 1H), 6.08 (d, 1H, J=4), 5.25 (m, 1H), 4.19-4.09 (m, 3H), 1.27-1.07 (m, 21H), 0.95-0.83 (m, 7H) ESI-MS: calc. 821.3 found 821.4

N^6,N^6, 2'O-tribenzoyl adenosine

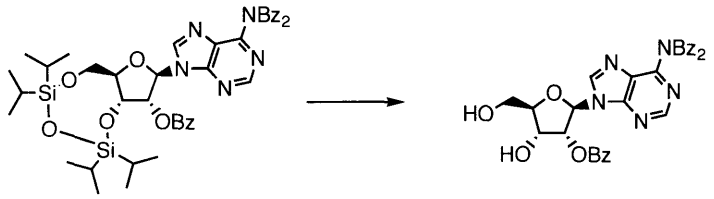

Several sets of cleavage conditions using various amine/HF and TBAF/THF systems were attempted. A dilute solution of 4:1 (v/v) TEA/HF in acetonitrile was found to cleave the silyl group completely within 1 hr at RT. The solution was then diluted with DCM and washed with 5% ammonium hydrogen carbonate to neutralize and remove remaining TEA/HF. Purification by silica column using 2:1, 1:1, 1:2 hexanes/ethyl acetate. ^{1}H-NMR (400 Mhz, CDCl3): δ 8.59 (s, 1H) 8.19 (s, 1H), 8.11-8.09 (m, 2H), 7.87-7.85 (m, 4H), 7.64-7.60 (m, 1H), 7.53-7.46 (m, 4H), 7.36-7.35 (m, 4H), 6.02 (d, 1H, J=7.6), 5.68 (d, 1H, J=5.6), 5.21 (dd, 1H, J=7.6, 5.2), 4.51 (s, 1H), 4.01-3.90 (m, 2H) ^{13}C-NMR (125 Mhz, CDCl3): δ 172.5, 166.4, 152.8, 151,152.0, 151.7, 145.2, 133.9, 133,5, 130.0, 129.7, 129.3, 129.1, 129.0, 128.8, 127.5, 91.3, 86.1, 75.3, 73.3, 63.1 ESI-MS: calc. 579.2 found 579.2

5'O-(t-butyl-dimethylsilyl)-N^6,N^6, 2'O-tribenzoyl-adenosine

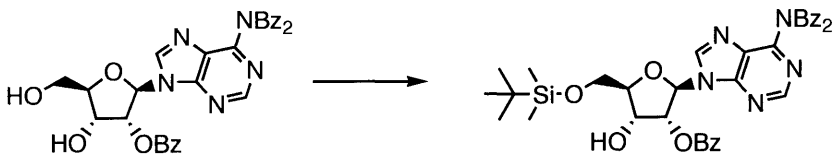

N^6,N^6, 2'O-tribenzoyl adenosine was dissolved in dry DMF under argon to which a freshly prepared solution of 1M TBDMS-Cl and 2M imidazole was added by syringe 1 eq at a time. The solution was stirred at RT overnight with additional TBDMS-Cl / imidazole solution added until completion was reached as determined by TLC. The solution was diluted with ethyl acetate and washed with brine several times. The organic phase was dried over Na_2SO_4 and concentrated *in vacuo*. The resulting syrup was purified over silica (0% to 33% ethyl acetate / hexanes). R_f (2:1 EtOAc / Hexanes) = 0.82 ^{1}H-NMR (500 Mhz, CDCl3): δ 8.65 (1H, s), 8.42 (1H, s), 8.15-8.13 (2H, m), 7.89-7.87 (4H, m), 7.64 (1H, m), 7.52-7,49 (4H, m), 7.40-7.36 (4H, m), 6.23 (1H, d, J=7 Hz), 5.67 (1H, dd, J_1= 5.5 Hz, J_2= 1.5 Hz), 4.99 (1H, dd, J_1= 7 Hz, J_2= 5.5 Hz), 4.52 (1H, dd, J_1= 4 Hz, J_2= 2.4 Hz), 3.95 (2H, m), 0.84 (9H, s), 0.09 (3H, s), 0.03 (3H, s) ESI-MS: calc 693.3 found 694.4

TBS-TBA-Phosphoramidite

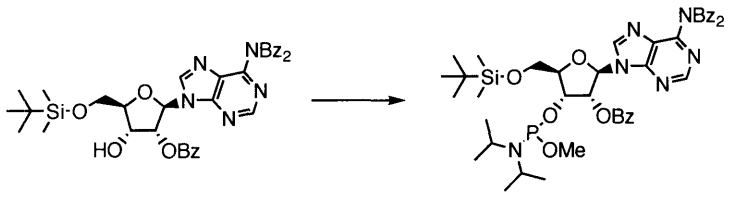

TBDMS-TBA and 2 eq. DCI were sealed in a dry flask with stirbar. The flask was evacuated and refilled with argon five times after which dry DCM was added by syringe and 2 eq. $(iPr_2N)_2POMe$. The reaction was stirred at RT and monitored by TLC (1:1 EtOAc / hexanes) with the product appearing at R_f = 0.79 and starting material at R_f = 0.32. Upon completion, the reaction was diluted with DCM, washed briefly with water to

remove the activator and dried over Na_2SO_4. Purification over silica using a gradient of 0 to 20% EtOAc in hexanes provided the product diastereomers as a colorless oil that foamed under vacuum. ^{1}H-NMR (300Mhz, $CDCl_3$) δ 8.69 (1H, d, J=6 Hz), 8.44 (1H, d, J=8 Hz), 8.16-8.10 (2H, m), 7.90-7.87 (4H, m), 7.64-7.57 (1H, m), 7.52-7.44 (4H, m) 7.39-7.33 (4H, m)6.43-6.36 (1H, m), 5.70-5.63 (1H, m), 5.12-5.00 (1H, m), 4.45-4.42 (1H, m), 4.01-3.98 (2H, m), 3.45-3.32 (2H, m), 3.18 and 2.90 (combined 3H, both d, J= 13 Hz), 1.00-0.81 (21H, m), 0.16-0.12 (6H, m)

6CFME-TBS-TBA

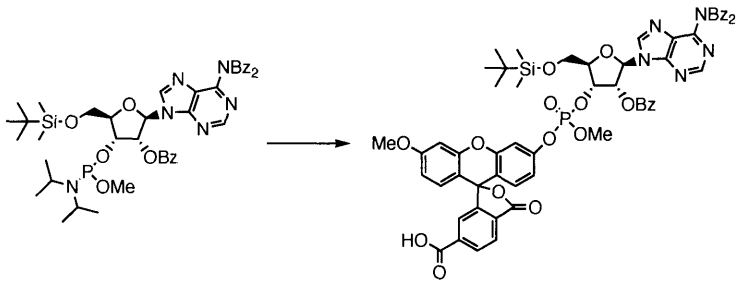

TBS-TBA-phosphoramidite, was sealed in a dry flask with 2 eq. DCI and 1.5 eq. 6CFME under dry argon. Dry, freshly distilled acetonitrile was added by syringe and the reaction stirred at RT for 30 min. The flask was then opened and 3 eq. of mCPBA added to oxidize the phosphite intermediate. After 30 min of oxidation, the solvent was removed *in vacuo* and the residue dissolved in DCM. The organic layer was washed with 1.5 M Na_2SO_3, 1M HCl and brine, then dried over Na_2SO_4. The crude mixture was purified over silica using 0-100% distilled THF in hexanes to provide an orange oil. ^{1}H-NMR (500 Mhz, $CDCl_3$) δ 8.69-8.63 (1H, m), 8.51-8.49 (1H, m), 8.32-8.20 (3H, m), 7.86-7.82 (4H, m), 7.60-7.51 (1H, m), 7.47-7.41 (4H, m), 7.36-7.33 (4H, m), 6.74-6.50 (6H, m), 5.80-5.70 (2H, m), 4.49 (1H, m), 4.05-3.95 (2H, m), 3.85-3.82 (3H, m), 3.67-3.64 (1H, m), 3.58-3.55 (1H, m), 0.93-0.91 (9H, m), 0.13-0.11 (6H, m)

TIPDS-N^6-benzoyl adenosine

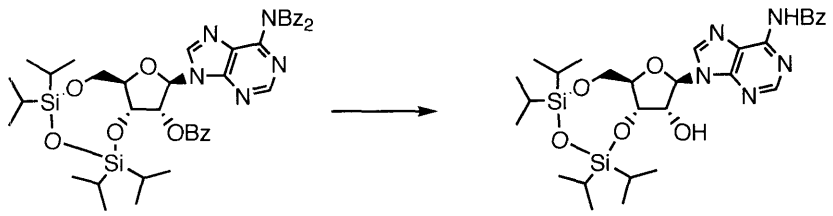

TIPDS-TBA (800 mg) was dissolved in 25 mL EtOH at 0 °C followed by the addition of 5 mL 25% (w/v) NaOMe / MeOH. The reaction was stirred on ice for 30 minutes before the reaction was terminated by the addition of 2 mL pyridine and 2 mL of glacial acetic acid to form a white slurry. The solvent was removed *in vacuo* and the residue dissolved in DCM. The organic layer was washed sat. $NaHCO_3$, and the aqueous layer was back-extracted twice with DCM. The combined organic layers were dried over $MgSO_4$ and purified over silica using a gradient of 0% to 4% MeOH in DCM. Removal of the solvent *in vacuo* yielded a white solid. 1H-NMR (300 Mhz, $CDCl_3$): δ 9.00 (s, 1H), 8.76 (s, 1H), 8.15 (s, 1H), 8.02 (d, 2H, J=7.2 Hz), 7.66-7.48 (m, 3H), 6.04 (s, 1H), 5.14 (dd, 1H, J=7.8, 5.4), 4.62 (d, 1H, J=5.4), 4.16-4.03 (m, 3H), 3.21 (s, 1H), 1.15-1.02 (m, 28H)

3'O-5'O-TIPDS-2'-6CFME-Adenosine

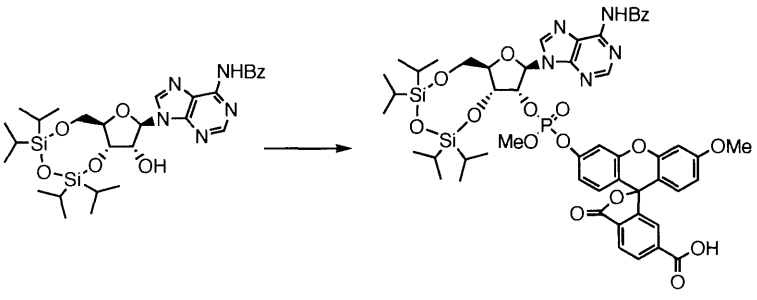

TIPDS-N^6-benzoyl adenosine and 2.6 eq. 4,5-dicyanoimidazole were combines in a dry flask with stirbar purged and filled with argon. Dry acetonitrile was added by syringe and the solids dissolved prior to the addition of 2.6 eq. $(iPr_2N)_2POMe$. The reaction stirred at

RT for 1 hour when TLC (EtOAc) showed complete consumption of the starting material. The solvent was removed *in vacuo* and the residue filtered through a silica plug with 1:1 EtOAc / hexanes to remove the activator and most of the phosphorodiamidite. The product was dried under vacuum prior to addition of 2.6 eq. DCI and 2 eq. 6CFME. The flask was purged with argon and dry acetonitrile was added by syringe. The solution stirred at RT for 1.5 hours before a solution of 5 eq. mCPBA in acetonitrile was added by syringe. Oxidation was allowed 40 minutes for completion before the solvent was removed *in vacuo*. The residue was dissolved in EtOAc, washed with 1.5M Na_2SO_3, 1M HCl, and brine and dried over Na_2SO_4.

2'-ACE-benzoyl adenosine

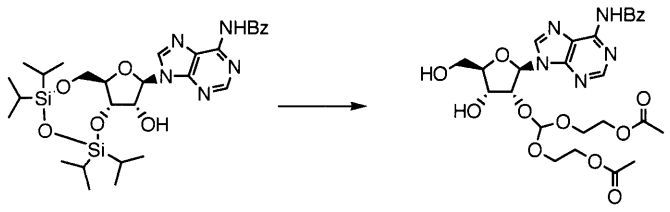

TIPDS-benzoyl adenosine was treated with ACE orthoester and catalytic PPTS under hi vacuum at 55 °C. PPTS was removed after neutralization with TMEDA by running the solution over a small column of silica with 1:1 EtOAc/Hexanes. Removal of solvent followed by treatment with 9:1 TMEDA/HF in acetonitrile to cleave the silyl groups yielded the desired product in 65% yield (2 steps)

^{1}H-NMR (300 Mhz, $CDCl_3$): δ 9.25 (bs, 1H), 8.76 (s, 1H), 8.08 (s, 1H), 8.03 (d, 2H, J=8.7 Hz), 7.62-7.43 (m, 3H), 6.00 (d, 1H, J=7.5 Hz), 5.21 (s, 1H), 5.09 (dd, 1H, J=7.2, 4.8 Hz), 4.51 (d, 1H, J=4.8 Hz), 4.23-4.15 (m, 1H) 4.07-3.42 (m, 11H), 2.06-2.02 (m, 6H) ESI-MS: calc. 589.2020 found 589.2009

5'TBS-2'ACE-benzoyl adenosine

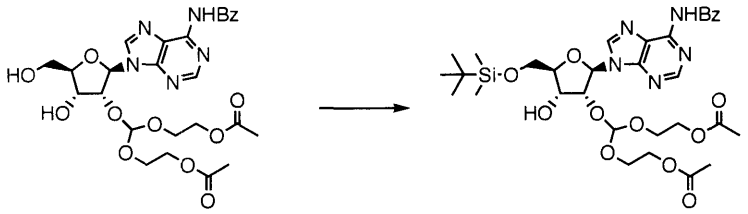

2'Ace-adenosine was reacted with 2 eq of imidazole and 1.1 eq of TBS-Cl in dry DMF. After stirring at room temperature overnight, a new spot on TLC appears at R_f=0.5 in 5% MeOH in EtOAc. This is of higher mobility than the starting material which near R_f=0.25. The reaction mixture was washed twice with water and once with brine, then dried over $MgSO_4$. Column purification yielded two fractions: one with R_f=0.5 and one that corresponds to recovered starting material. Obtained product in 37% yield and recovered 34% starting material. ^{1}H-NMR: δ (ppm) 9.15 (bs, 1H), 8.80 (s, 1H), 8.40 (s, 1H), 8.03 (d, 2H), 7.55 (dt, 3H), 6.32 (d, 1H), 5.40 (s, 1H), 4.87 (t, 1H), 4.43 (q, 1H), 4.23-3.47 (m, 11H), 3.02 (bs, 1H), 2.02, (d, 6H), 0.92 (s, 9H), 0.12 (d, 6H)

5'TBS-3' diisopropyl methoxyphosphoramidite-2'ACE-benzoyl adenosine

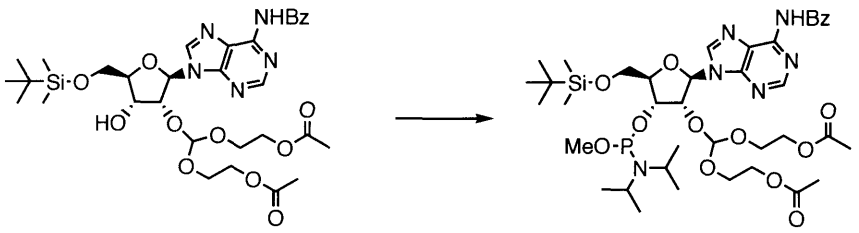

5'TBS-2'ACE-benzoyl adenosine was combined with dicyanoimidazole (1 eq) in a dry round bottom flask and sealed with a rubber septum. The flask was placed under hi-vac for 30 minutes followed by 5 fill-purge cycles with nitrogen. 1 mL of freshly distilled dry DCM was then added by syringe followed by tetraisopropyl methoxy phosphordiamidite. The reaction was allowed to stir at room temperature and was monitored by TLC using 2:1 EtOAc/Hexanes. The solvent was removed in vacuo and the

compound purified over silica using 1:1 EtOAc/Hexanes. Overnight drying on hi-vac yielded a clear oil in 28% yield. .

^{1}H-NMR: δ (ppm) 9.06 (bs, 1H), 8.80 (s, 1H), 8.41 (s, 1H), 8.03 (d, 2H), 7.56 (dt, 3H), 6.33 (m, 1H), 5.46 (s, 1H), 4.9-3.8 (m, 18H), 2.01 (d, 6H), 1.25-1.17 (m, 12H), 0.94 (9H), 0.11 (6H) ^{31}P-NMR: δ (ppm) 148

TIPDS-THP-NBz-Adenosine

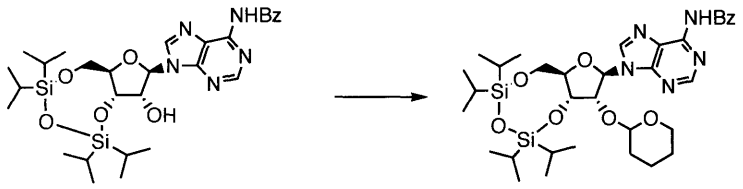

TIPDS-NBz-Adenosine (500 mg, 0.81 mmol) was dissolved in DCM with TsOH (154 mg, 0.81 mmol). Dihydropyran (274 mg, 3.26 mmol) was then added and the solution stirred at RT for 6 hours at which point ESI-MS showed complete consumption of the starting material. The reaction was diluted with DCM, washed with sat. $NaHCO_3$ and brine, and dried over Na_2SO_4. The crude product was purified over silica using 0% to 2% MeOH in DCM to yield an oil in quantitative yield. ^{1}H-NMR (300 Mhz, $CDCl_3$) δ 9.16 (1H, s), 8.77 and 8.74 (1H, s), 8.35 and 8.23 (1H, s), 8.01 (2H, d, J=7 Hz), 7.58-7.47 (3H, m), 6.14 and 6.10 (1H, s), 5.32-3.49 (8H, m), 1.88-1.40 (6H, m),1.09-0.97 (28H, m) ESI-MS $[M+H]^{+}$ 698.3

THP-NBz-adenosine

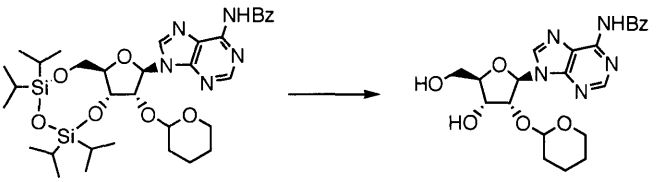

TIPDS-THP-NBz-Aden (350 mg, 0.5 mmol) was dissolved in 4 mL acetonitrile in a polypropylene tube followed by the addition of 0.5 mL 4:1 (v/v) TEA/HF. The reaction

was monitored by TLC (5% MeOH / EtOAc) for 4 hours at RT. The reaction was then diluted with DCM, washed with 5% NH_4HCO_3 and brine, and dried over Na_2SO_4. The crude was purified over silica using 50% to 100% EtOAc in hexanes followed by 5% MeOH in EtOAc to elute the product as an off-white solid in 44% yield. . ^{1}H-NMR (400 Mhz, $CDCl_3$) δ 8.81 (1H, s), 8.09 (1H, s), 8.05 (2H, dd, J_a = 7 Hz, J_b = 2 Hz), 7.62 (1H, t, J = 7 Hz), 7.54 (2H, dt, J_a = 8 Hz J_b = 2 Hz), 6.04 and 5.99 (1H, d, J= 7 Hz), 5.11 and 4.89 (1H, dd, J_a = J_b = 8 Hz), 4.6-4.56 (1H, m), 4.43-4.38 (2H, m), 4.03 and 4.02 (1H, s), 3.80 (1H, t, J = 11 Hz), 3.50-2.95 (2H, m), 1.85-1.60 (2H, m), 1.55-1.32 (4H, m) ESI-MS $[M+H]^+$ 456.2

TBS-THP-NBz-Adenosine

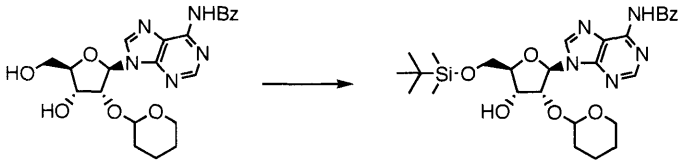

THP-NBz-Adenosine (55 mg, 0.12 mmol) was dissolved in 5 mL dry DMF under argon. 0.15 mL of a freshly prepared solution of 1M TBDMS-Cl and 2M imidazole in dry DMF was added by syringe and the reaction stirred at RT overnight. ESI-MS showed both product and starting material peaks. An additional 0.2 mL of the TBDMS-Cl/imidazole solution was added each hour until completion. The reaction was diluted with EtOAc, washed with water and brine, and dried over Na_2SO_4. Purification over silica using a gradient of 0% to 100% EtOAc in hexanes provided the product in 96% yield. ^{1}H-NMR (500 Mhz, $CDCl_3$) δ 8.83 and 8.82 (1H, s), 8.46 and 8.39 (1H, s), 8.04 (2H, dd, J_a = 7 Hz J_b = 2 Hz), 7.60 (1H, t, J = 8 Hz), 7.52 (2H, d, J=8 Hz), 6.39 and 6.28 (1H, d, J = 6 Hz), 4.84-3.15 (8H, m), 1.84-1.31 (6H, m), 0.94 and 0.93 (9H, s), 0.13-0.11 (6H, m) ^{13}C-NMR (125 MHz, $CDCl_3$) δ 152.8, 151.8, 149.6, 141.9, 141.6, 133.9, 133.0, 129.0, 128.1, 123.3, 123.1, 101.7, 99.9, 87.2, 86.8, 85.7, 85.5, 82.5, 79.9, 70.7, 70.2, 65.4, 63.4, 63.3, 63.1, 31.0, 30.4, 26.2, 25.0, 21.0, 19.6, 19.4, 18.7, 18.6, -5.10, -5.14, -5.29, -5.30 ESI-MS $[M+H]^+$ 570.3

6CFME-TBS-THP-NBz-Adenosine

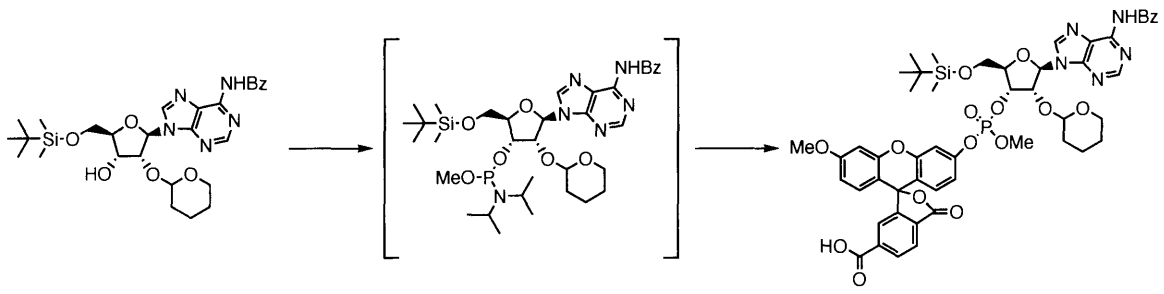

TBS-THP-NBz-Adenosine (250 mg, 0.44 mmol) was combined with DCI (104 mg, 0.88 mmol) in a dry flask with stirbar. The flask was evacuated and refilled with argon four times to remove oxygen and atmospheric moisture. Dry acetonitrile (10 mL) was added by syringe and the solution stirred at RT to dissolve the solids. $(iPr_2N)_2POMe$ (288 mg, 1.1 mmol) was then added by syringe. Reaction progress was monitored by ESI-MS with comple consumption of starting material observed at 15-20 minutes. The solvent was then removed *in vacuo*, the residue filtered through a silica plug using 1:1 EtOAc / hexanes, and dried under vacuum to a white foam. 6CFME (242 mg, 0.63 mmol) and DCI (104 mg, 0.88 mmol) were added and the flask purged with nitrogen. Dry acetonitrile (10 mL) was added by syringe and the reaction stirred at RT. At 40 minutes, complete consumtion of the phosphoramidite was confirmed by ESI-MS. The phosphite was oxidized to the phosphate by the addition of mCPBA (430 mg, 1.76 mmol, 70% by mass) and stirring at RT for 20 min. The product was purified by semi-prep HPLC using a gradient of 25% to 85% acetonitrile in water and monitored at 254 nm. The product eluted at 18 min. ESI-MS $[M+H]^+$ 1036.3

6CFME-TBS-THP-NBz-Adenosine-POMe

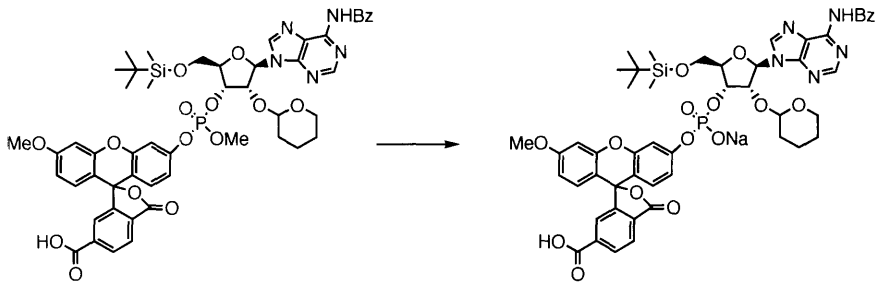

The starting material was dissolved in DMF containing 1M disodium-2-carbamoyl-2-cyanoethylene-1,1-dithiolate trihydrate (S2Na2) and stirred at ambient temperature for 2 hours. The solution was then diluted with 1:1 acetonitrile / water and purified by reverse-phase HPLC using a gradient of 25% to 85% acetonitrile in water over 20 minutes with a flow rate of 4 mL / min. The elution of the compound was monitored by UV absorbance at 254 nm and appeared with an elution time of 14 minutes. The product was then lyophilized to an off-white powder. ESI-MS $[M+H]^+$ 1022.3

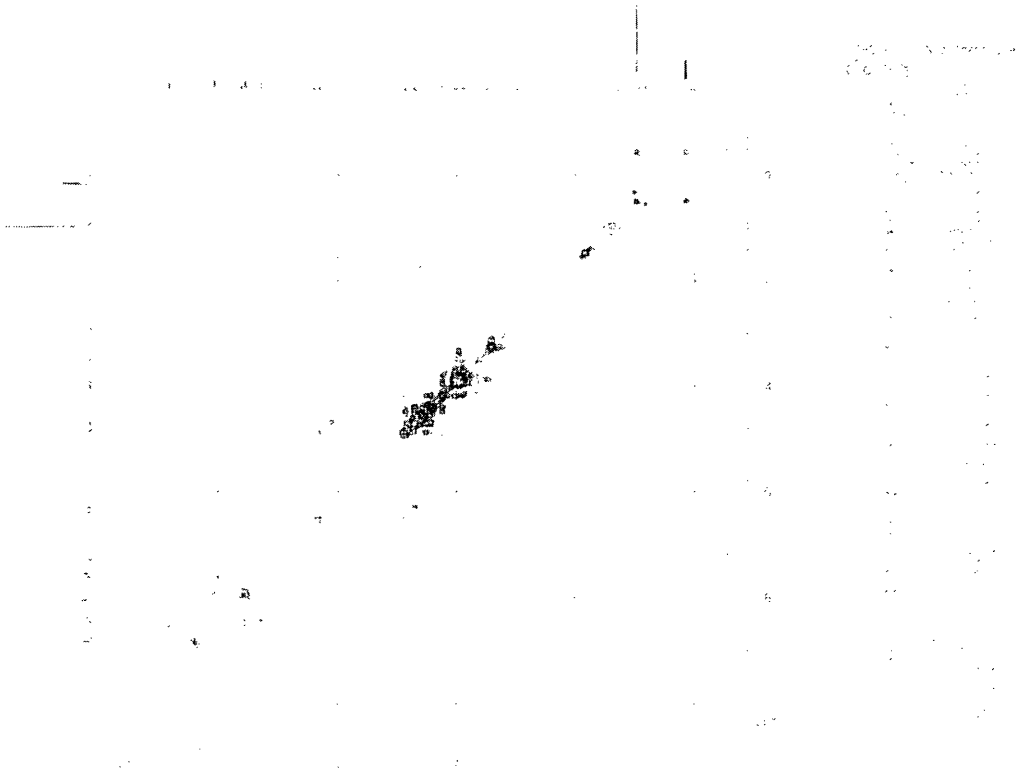

1

H-^{1}H COSY of 6CFME-5'O-TBS-3'O-THP-N^{6}Bz-Adenosine

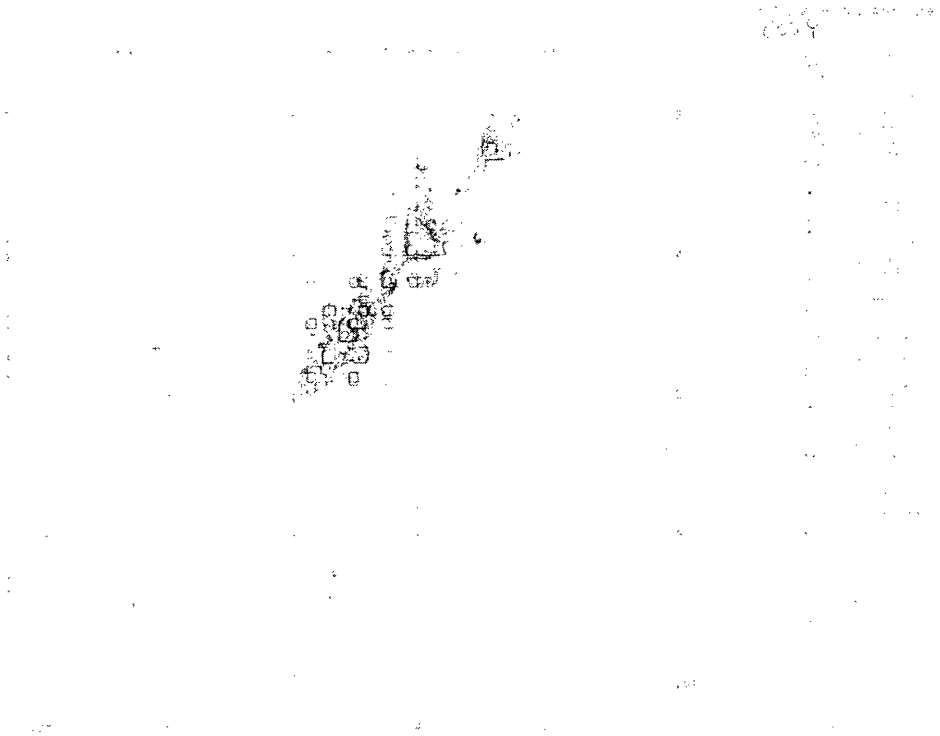

Expansion of ^{1}H-^{1}H COSY of 6CFME-5'O-TBS-3'O-THP-N^{6}Bz-Adenosine